


SOURCE  
DATATRANSPARENT  
PROCESSOPEN  
ACCESS

# $\beta$ -RA reduces DMQ/CoQ ratio and rescues the encephalopathic phenotype in *Coq9*<sup>R239X</sup> mice

Agustín Hidalgo-Gutiérrez<sup>1,2</sup>, Eliana Barriocanal-Casado<sup>1,2</sup>, Mohammed Bakkali<sup>3</sup>, M Elena Díaz-Casado<sup>1,2</sup>, Laura Sánchez-Maldonado<sup>1,2</sup>, Miguel Romero<sup>4</sup>, Ramy K Sayed<sup>2,5</sup>, Cornelia Prehn<sup>6</sup>, Germaine Escames<sup>1,2,7</sup>, Juan Duarte<sup>4</sup>, Darío Acuña-Castroviejo<sup>1,2,7</sup> & Luis C López<sup>1,2,7,\*</sup> 

## Abstract

Coenzyme Q (CoQ) deficiency has been associated with primary defects in the CoQ biosynthetic pathway or to secondary events. In some cases, the exogenous CoQ supplementation has limited efficacy. In the *Coq9*<sup>R239X</sup> mouse model with fatal mitochondrial encephalopathy due to CoQ deficiency, we have tested the therapeutic potential of  $\beta$ -resorcylic acid ( $\beta$ -RA), a structural analog of the CoQ precursor 4-hydroxybenzoic acid and the anti-inflammatory salicylic acid.  $\beta$ -RA noticeably rescued the phenotypic, morphological, and histopathological signs of the encephalopathy, leading to a significant increase in the survival. Those effects were due to the decrease of the levels of demethoxyubiquinone-9 (DMQ<sub>9</sub>) and the increase of mitochondrial bioenergetics in peripheral tissues. However, neither CoQ biosynthesis nor mitochondrial function changed in the brain after the therapy, suggesting that some endocrine interactions may induce the reduction of the astrogliosis, spongiosis, and the secondary down-regulation of astrocytes-related neuroinflammatory genes. Because the therapeutic outcomes of  $\beta$ -RA administration were superior to those after CoQ<sub>10</sub> supplementation, its use in the clinic should be considered in CoQ deficiencies.

**Keywords** 2,4-dihydroxybenzoic acid; astrogliosis; mitochondrial encephalopathy; Q synthome; spongiosis

**Subject Categories** Genetics, Gene Therapy & Genetic Disease; Pharmacology & Drug Discovery

**DOI** 10.15252/emmm.201809466 | Received 23 June 2018 | Revised 23 October 2018 | Accepted 26 October 2018

**EMBO Mol Med (2018) e9466**

## Introduction

Mitochondria are the primary site of cellular energy production and can also have a broad range of other vital functions for the cells. Dysfunction of mitochondria is observed in common age-related disorders, including neurodegenerative diseases, metabolic syndrome, cardiomyopathies, and sarcopenia (Nunnari & Suomalainen, 2012). Mitochondrial dysfunction is likewise the primary characteristic of monogenic disorders that affect one of the genes that encode the estimated 1,000 proteins identified in mitochondria (Pagliarini *et al*, 2008). Among these, mutations in genes encoding essential proteins for the oxidative phosphorylation (OXPHOS) system account for the most common group of inborn errors of metabolism. The therapeutic options for these disorders are mostly limited to palliative care and remain woefully inadequate (DiMauro *et al*, 2013; Wang *et al*, 2016).

Primary deficiency of coenzyme Q10 (CoQ<sub>10</sub>), due to CoQ<sub>10</sub> biosynthetic defects, is a mitochondrial syndrome that affects the OXPHOS system, and it has heterogeneous clinical presentations and variable response to therapy with exogenous CoQ<sub>10</sub> (DiMauro *et al*, 2007; Emmanuele *et al*, 2012). To understand the disease mechanisms, we previously generated and characterized the first mouse model of mitochondrial encephalopathy due to CoQ deficiency. The mouse model presents two point mutations, leading to a premature stop codon in *Coq9* (*Coq9*<sup>R239X</sup>; Garcia-Corzo *et al*, 2013). These mutations are homologues to the mutations identified in a patient (*COQ9*<sup>R244X</sup>; Duncan *et al*, 2009). The resulting dysfunctional COQ9 protein causes a profound reduction in the levels of COQ7 protein and disruption of the multiprotein complex for CoQ biosynthesis (Complex Q), resulting in a severe CoQ deficiency with accumulation of demethoxyubiquinone (DMQ = 2-polyprenyl-6-methoxy-3-methyl-1,4-benzoquinone), brain mitochondrial dysfunction, oxidative damage, disruption of sulfide

<sup>1</sup> Departamento de Fisiología, Facultad de Medicina, Universidad de Granada, Granada, Spain

<sup>2</sup> Instituto de Biotecnología, Centro de Investigación Biomédica, Universidad de Granada, Granada, Spain

<sup>3</sup> Departamento de Genética, Facultad de Ciencias, Universidad de Granada, Granada, Spain

<sup>4</sup> Departamento de Farmacología, Facultad de Farmacia, Universidad de Granada, Granada, Spain

<sup>5</sup> Department of Anatomy and Embryology, Faculty of Veterinary Medicine, Sohag University, Sohag, Egypt

<sup>6</sup> Institute of Experimental Genetics, Genome Analysis Center, Helmholtz Zentrum München, Neuherberg, Germany

<sup>7</sup> Centro de Investigación Biomédica en Red de Fragilidad y Envejecimiento Saludable (CIBERFES), Granada, Spain

\*Corresponding author. Tel: +34 958241000 ext. 20197; E-mail: luisca@ugr.es

metabolism, reactive astrogliosis, spongiform degeneration, hypotension, and premature death (Garcia-Corzo *et al*, 2013; Luna-Sanchez *et al*, 2017). These pathological features are similar to those described in patients with mutations in *COQ7* and *COQ9*, who presented a severe early-onset multisystemic disease dominated by encephalopathy, the phenotype associated with CoQ deficiency with the most limited response to oral CoQ<sub>10</sub> supplementation (Lopez *et al*, 2006; Duncan *et al*, 2009; Emmanuele *et al*, 2012; Danhauser *et al*, 2016; Smith *et al*, 2018).

Consistent with the poor therapeutic effects of CoQ supplementations in patients, oral supplementation with ubiquinone-10, the oxidized form of CoQ<sub>10</sub>, was ineffective in the *Coq9*<sup>R239X</sup> mouse model due to its poor absorption and bioavailability, which is more accused in the CNS because of the presence of the blood brain barrier (Bentinger *et al*, 2003; Bhagavan & Chopra, 2007; Lopez *et al*, 2010; Garcia-Corzo *et al*, 2014). The supplementation with ubiquinol-10, the reduced form of ubiquinone-10, provided better therapeutic outcomes because it induced slight improvements in mitochondrial bioenergetics in the brain and reduction of the oxidative stress and astrogliosis (Garcia-Corzo *et al*, 2014).

An alternative strategy to the exogenous CoQ<sub>10</sub> supplementation is to increase the endogenous CoQ biosynthesis. The biosynthesis of CoQ<sub>10</sub> occurs in a complex biosynthetic pathway in which the 4-hydroxybenzoic acid (4-HB) is the initial substrate. This precursor of the benzoquinone ring of CoQ is first prenylated, and then, a total of seven reactions (one decarboxylation, three hydroxylation, and three methylation) produce the fully substituted benzoquinone ring of CoQ (Fig EV1; Kawamukai, 2016). One of the hydroxylation steps is catalyzed by COQ7, a hydroxylase that needs another protein, COQ9, for its stability and normal function (Garcia-Corzo *et al*, 2013; Lohman *et al*, 2014). The hydroxyl group incorporated by COQ7 into the benzoquinone ring is already present in the molecule  $\beta$ -resorcylic acid ( $\beta$ -RA), also named 2,4-hydroxybenzoic acid (2,4-diHB). Therefore,  $\beta$ -RA is a 4-HB analog that can be theoretically used in the CoQ biosynthesis pathway in order to bypass a defect from the hydroxylation step catalyzed by COQ7 (Fig EV1). This strategy was partially successful *in vitro* in *COQ7* null yeasts, as well as in mouse and human fibroblasts with mutations in *COQ7* or *COQ9* (Xie *et al*, 2012; Freyer *et al*, 2015; Luna-Sanchez *et al*,

2015). Additionally,  $\beta$ -RA is a structural analogue of salicylic acid (2-hydroxybenzoic acid), an anti-inflammatory molecule that may be potentially valuable to reduce the neuroinflammation (Lan *et al*, 2011; Gomez-Guzman *et al*, 2014), a factor that has been recently postulated as an essential pathomechanism and a therapeutic target in mitochondrial encephalopathies (Ignatenko *et al*, 2018), leukoencephalopathy, and neurodegenerative diseases (Eto *et al*, 2002; Liddelow & Barres, 2015, 2017). Also salicylic derivative, known as salicylates, may act as mTOR inhibitors (Cameron *et al*, 2016), and this action may be therapeutic in mitochondrial diseases (Johnson *et al*, 2013).

Based on the properties of  $\beta$ -RA, we have evaluated its therapeutic potential in a mouse model of mitochondrial encephalopathy due to CoQ deficiency. Our data show novel therapeutic mechanisms and represent one of the few cases of successful therapies for mitochondrial encephalopathies that could easily be implemented into the clinic.

## Results

### The treatment with $\beta$ -RA rescues the phenotype of *Coq9*<sup>R239X</sup> mice

We previously demonstrated that *Coq9*<sup>R239X</sup> mice have reduced size and body weight, and die between 3 and 7 months of age (Garcia-Corzo *et al*, 2013). Moreover, we proved that ubiquinol-10 treatment induces biochemical and histopathological improvements in the brain of *Coq9*<sup>R239X</sup> mice (Garcia-Corzo *et al*, 2014). These improvements led to a significant increase in the survival of *Coq9*<sup>R239X</sup> mice treated with ubiquinol-10, compared to the *Coq9*<sup>R239X</sup> mice. While the *Coq9*<sup>R239X</sup> mice reached a maximum age of 7 months, with a median survival of 5 months of age, the *Coq9*<sup>R239X</sup> mice treated with ubiquinol-10 reached a maximum age of 17 months, with a median survival of 13 months of age (Fig 1A). Interestingly, the therapeutic effect of oral  $\beta$ -RA supplementation resulted in an even greater increase in the survival of *Coq9*<sup>R239X</sup> mice, reaching a maximum lifespan of 25 months of age, with a median survival of 22 months of age (Fig 1A). Therefore, the extension in the lifespan achieved by  $\beta$ -RA in *Coq9*<sup>R239X</sup> mice reached values close to the lifespan in wild-type mice (Fig 1A).

**Figure 1. Survival and phenotypic characterization of *Coq9*<sup>R239X</sup> mice after  $\beta$ -RA treatment.**

- A Survival curve of the *Coq9*<sup>+/+</sup> mice, *Coq9*<sup>R239X</sup> mice, and *Coq9*<sup>R239X</sup> mice after  $\beta$ -RA treatment and *Coq9*<sup>R239X</sup> after ubiquinol-10 treatment. The treatments started at 1 month of age [Log-rank (Mantel-Cox) test or Gehan-Breslow-Wilcoxon test; *Coq9*<sup>+/+</sup>, *n* = 9; *Coq9*<sup>R239X</sup>, *Coq9*<sup>R239X</sup> after  $\beta$ -RA treatment, and *Coq9*<sup>R239X</sup> after ubiquinol-10 treatment, *n* = 15 for each group].
- B Survival curve of the *Coq9*<sup>R239X</sup> mice and *Coq9*<sup>R239X</sup> mice after  $\beta$ -RA treatment started at 3 months of age (*Coq9*<sup>R239X</sup>, *n* = 15; *Coq9*<sup>R239X</sup> after  $\beta$ -RA treatment, *n* = 10).
- C, D Body weight of males (C) and females (D) *Coq9*<sup>+/+</sup> mice, *Coq9*<sup>R239X</sup> mice, and *Coq9*<sup>R239X</sup> mice after  $\beta$ -RA treatment [(C): *Coq9*<sup>+/+</sup>, *n* = from 31 to 4; *Coq9*<sup>R239X</sup>, *n* = from 13 to 13; *Coq9*<sup>R239X</sup> after  $\beta$ -RA treatment, *n* = from 31 to 7. (D): *Coq9*<sup>+/+</sup>, *n* = from 22 to 3; *Coq9*<sup>R239X</sup>, *n* = from 13 to 12; *Coq9*<sup>R239X</sup> after  $\beta$ -RA treatment, *n* = from 24 to 3].
- E, F Rotarod test of male (E) and female (F) *Coq9*<sup>+/+</sup> mice, *Coq9*<sup>R239X</sup> mice, and *Coq9*<sup>R239X</sup> mice after  $\beta$ -RA treatment [(E): *Coq9*<sup>+/+</sup>, *n* = from 11 to 8; *Coq9*<sup>R239X</sup>, *n* = from 10 to 10; *Coq9*<sup>R239X</sup> after  $\beta$ -RA treatment, *n* = from 11 to 9. (F): *Coq9*<sup>+/+</sup>, *n* = from 5 to 5; *Coq9*<sup>R239X</sup>, *n* = from 4 to 4; *Coq9*<sup>R239X</sup> after  $\beta$ -RA treatment, *n* = from 11 to 6].
- G Blood pressure of *Coq9*<sup>+/+</sup> mice, *Coq9*<sup>R239X</sup> mice, and *Coq9*<sup>R239X</sup> mice after  $\beta$ -RA treatment. Data from male and female mice are represented together (*Coq9*<sup>+/+</sup>, *n* = 6; *Coq9*<sup>R239X</sup>, *n* = 6; *Coq9*<sup>R239X</sup> after  $\beta$ -RA treatment, *n* = 7). The whiskers down and up of the boxes indicate the minimum and maximum value, respectively. Horizontal lines inside the boxes mark the median.
- H Comparative image of a *Coq9*<sup>R239X</sup> mouse and a *Coq9*<sup>R239X</sup> mouse after  $\beta$ -RA treatment at 4 months of age.

Data information: Data are expressed as mean  $\pm$  SD. \**P* < 0.05; \*\**P* < 0.01; \*\*\**P* < 0.001; *Coq9*<sup>R239X</sup> or *Coq9*<sup>R239X</sup> after  $\beta$ -RA treatment versus *Coq9*<sup>+/+</sup>. +*P* < 0.05; ++*P* < 0.01; *Coq9*<sup>R239X</sup> versus *Coq9*<sup>R239X</sup> after  $\beta$ -RA treatment (one-way ANOVA with a Tukey's *post hoc* test or t-test; see Appendix Table S2 for exact *P*-values).

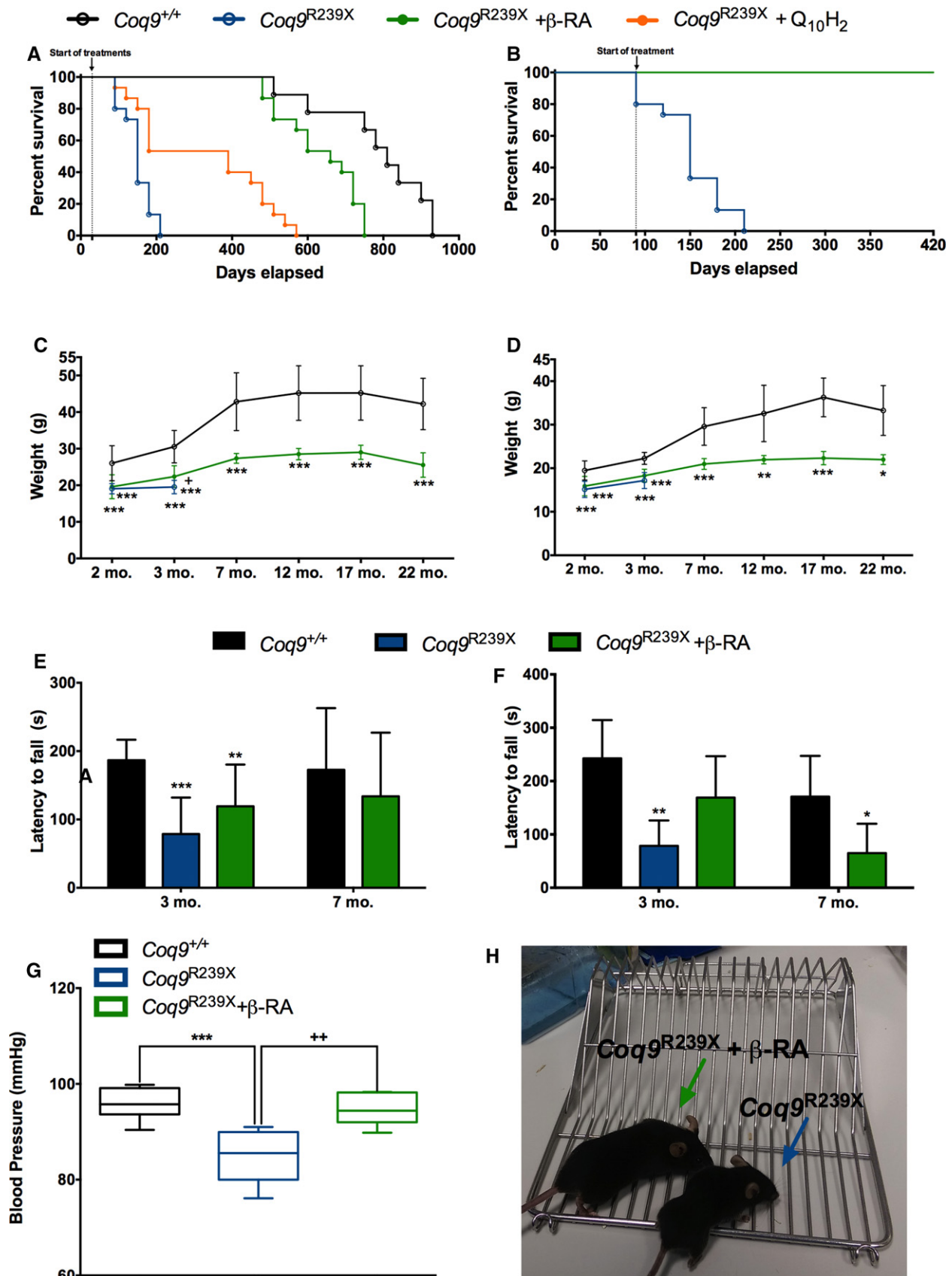


Figure 1.

Analysis using the log-rank (Mantel-Cox) and the Gehan–Breslow–Wilcoxon tests shows significant differences ( $P < 0.0001$  and  $P = 0.0017$ , respectively) between *Coq9*<sup>+/+</sup> mice, *Coq9*<sup>R239X</sup> mice, *Coq9*<sup>R239X</sup> mice treated with  $\beta$ -RA, and *Coq9*<sup>R239X</sup> mice treated with ubiquinol-10 (Fig 1A). Moreover, if the  $\beta$ -RA treatment started at 3 months of age (symptomatic period) instead of 1 month of age (asymptomatic period), 100% of the treated mice remained alive at 14 months of age (Fig 1B).

The striking increase in survival was in parallel of/accompanied by a phenotypic improvement. *Coq9*<sup>R239X</sup> mice treated with  $\beta$ -RA showed a slight increase in the body weight, although the values did not reach the wild-type levels (Fig 1C and D). The motor coordination tested by rotarod assay showed a decrease in the latency to fall in *Coq9*<sup>R239X</sup> mice compared to *Coq9*<sup>+/+</sup> mice. The treatment with  $\beta$ -RA significantly attenuated the motor phenotype in *Coq9*<sup>R239X</sup> mice, both

in males and females (Fig 1E and F). The treatment also normalized the blood pressure (Fig 1G), while the blood cells and hemoglobin levels did not change in the experimental groups (Appendix Fig S1). The general health improvement of *Coq9*<sup>R239X</sup> mice treated with  $\beta$ -RA was remarkable, clearly showing a healthier demeanor, compared to the untreated *Coq9*<sup>R239X</sup> mice (Fig 1H and Movie EV1).

#### The treatment with $\beta$ -RA induces a reduction in the histopathological signs of the encephalopathy

Because of the striking effect of the treatment on the survival and health status of the *Coq9*<sup>R239X</sup> mice, we performed a histopathological evaluation of the brain, the main symptomatic tissue. The spongiform degeneration and reactive astrogliosis characteristic in the diencephalon (Fig 2B<sub>1</sub>, E<sub>1</sub>, H<sub>1</sub>, and K<sub>1</sub>) and

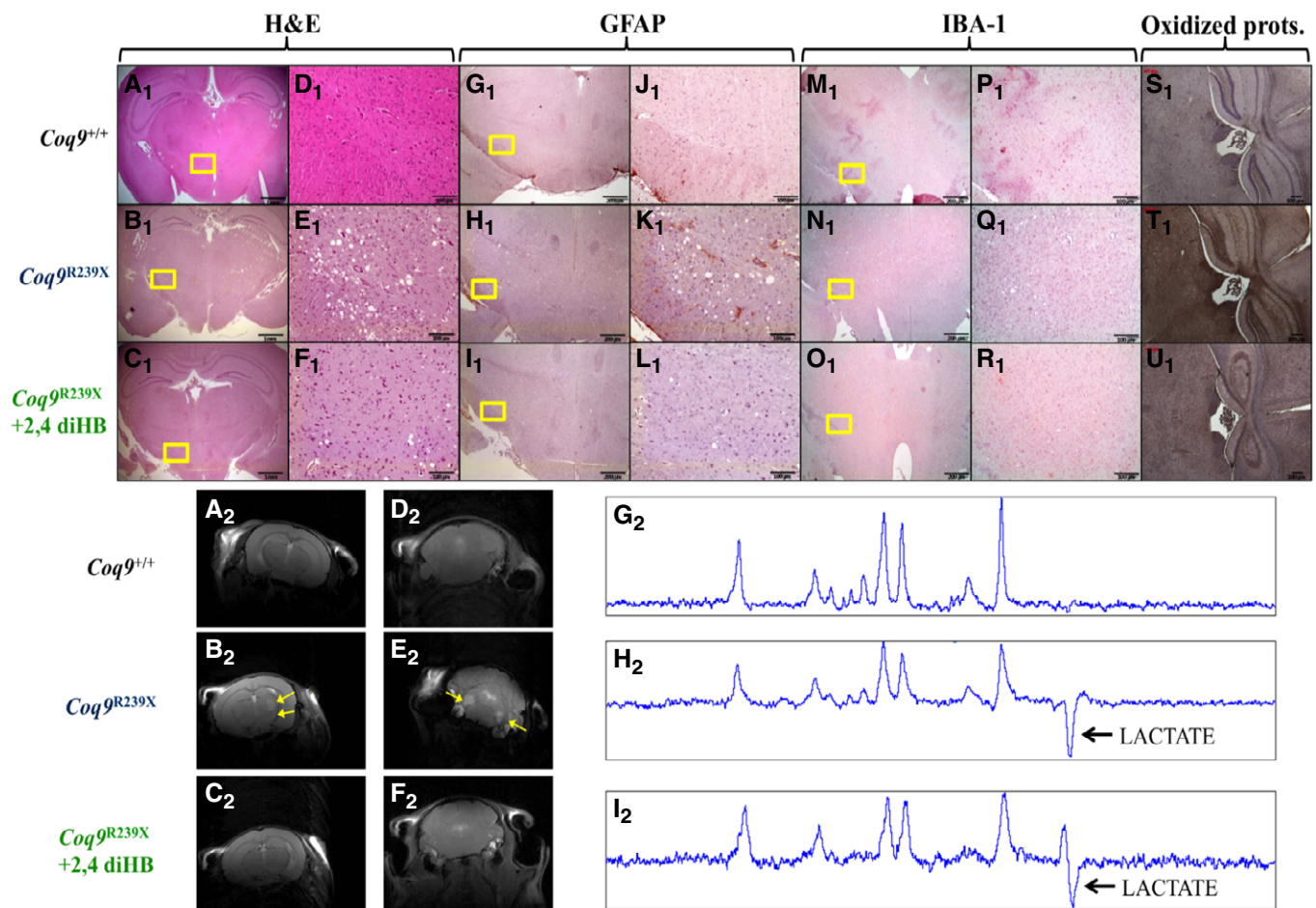


**Figure 2. Pathological features in the brain of *Coq9*<sup>R239X</sup> mice after  $\beta$ -RA treatment.**

A–U (A<sub>1</sub>–F<sub>1</sub>) H&E stain in the diencephalon of *Coq9*<sup>+/+</sup> mice (A<sub>1</sub> and D<sub>1</sub>), *Coq9*<sup>R239X</sup> mice (B<sub>1</sub> and E<sub>1</sub>), and *Coq9*<sup>R239X</sup> mice after  $\beta$ -RA treatment (C<sub>1</sub> and F<sub>1</sub>). (G<sub>1</sub>–L<sub>1</sub>) Anti-GFAP stain in the diencephalon of *Coq9*<sup>+/+</sup> mice (G<sub>1</sub> and J<sub>1</sub>), *Coq9*<sup>R239X</sup> mice (H<sub>1</sub> and K<sub>1</sub>), and *Coq9*<sup>R239X</sup> mice after  $\beta$ -RA treatment (I<sub>1</sub> and L<sub>1</sub>). (M<sub>1</sub>–R<sub>1</sub>) Anti-Iba1 stain in the diencephalon of *Coq9*<sup>+/+</sup> mice (M<sub>1</sub> and P<sub>1</sub>), *Coq9*<sup>R239X</sup> mice (N<sub>1</sub> and Q<sub>1</sub>), and *Coq9*<sup>R239X</sup> mice after  $\beta$ -RA treatment (O<sub>1</sub> and R<sub>1</sub>). (S<sub>1</sub>–U<sub>1</sub>) Protein oxidation in the diencephalon of *Coq9*<sup>+/+</sup> mice (S<sub>1</sub>), *Coq9*<sup>R239X</sup> mice (T<sub>1</sub>), and *Coq9*<sup>R239X</sup> mice after  $\beta$ -RA treatment (U<sub>1</sub>). (A<sub>2</sub>–C<sub>2</sub>) Magnetic Resonance Images of the diencephalon of *Coq9*<sup>+/+</sup> mice (A<sub>2</sub>), *Coq9*<sup>R239X</sup> mice (B<sub>2</sub>), and *Coq9*<sup>R239X</sup> mice after  $\beta$ -RA treatment (C<sub>2</sub>). (D<sub>2</sub>–F<sub>2</sub>) Magnetic Resonance Images of the pons of *Coq9*<sup>+/+</sup> mice (D<sub>2</sub>), *Coq9*<sup>R239X</sup> mice (E<sub>2</sub>), and *Coq9*<sup>R239X</sup> mice after  $\beta$ -RA treatment (F<sub>2</sub>). (G<sub>2</sub>–I<sub>2</sub>) Lactate peak in the brain of *Coq9*<sup>+/+</sup> mice (G<sub>2</sub>), *Coq9*<sup>R239X</sup> mice (H<sub>2</sub>), and *Coq9*<sup>R239X</sup> mice after  $\beta$ -RA treatment (I<sub>2</sub>). Scale bars: 1 mm (A<sub>1</sub>–C<sub>1</sub>); 100  $\mu$ m (D<sub>1</sub>–F<sub>1</sub>); 200  $\mu$ m (G<sub>1</sub>–L<sub>1</sub>); 100  $\mu$ m (J<sub>1</sub>–L<sub>1</sub>); 200  $\mu$ m (M<sub>1</sub>–O<sub>1</sub>); 100  $\mu$ m (P<sub>1</sub>–R<sub>1</sub>); 100  $\mu$ m (S<sub>1</sub>–U<sub>1</sub>). The yellow arrows indicated the areas of increased T2 signal, which is characteristic of lesions in specific brain areas.

the pons (Appendix Fig S2) of the *Coq9*<sup>R239X</sup> mice (García-Corzo *et al*, 2013), compared to *Coq9*<sup>+/+</sup> mice (Fig 2A<sub>1</sub>, D<sub>1</sub>, G<sub>1</sub>, and J<sub>1</sub>; Appendix Fig S2), almost disappeared after the  $\beta$ -RA treatment (Fig 2C<sub>1</sub>, F<sub>1</sub>, I<sub>1</sub>, and L<sub>1</sub>; Appendix Fig S2). The microglia distribution did not show any difference between the three experimental groups (Fig 2M<sub>1</sub>–R<sub>1</sub>; Appendix Fig S2). Moreover, the increased protein oxidation observed in the diencephalon of *Coq9*<sup>R239X</sup> mice (Fig 2T<sub>1</sub>), compared to *Coq9*<sup>+/+</sup> mice (Fig 2S<sub>1</sub>), was attenuated in *Coq9*<sup>R239X</sup> mice treated with  $\beta$ -RA (Fig 2U<sub>1</sub>).

The improvements in the histopathological features were further corroborated by magnetic resonance imaging (MRI). Brain injuries were observed in the diencephalon and the pons of *Coq9*<sup>R239X</sup> mice (Fig 2B<sub>2</sub>–E<sub>2</sub>; Appendix Fig S2). In *Coq9*<sup>+/+</sup> mice and *Coq9*<sup>R239X</sup> mice treated with  $\beta$ -RA, however, we did not detect any sign of brain injury (Fig 2A<sub>2</sub>, D<sub>2</sub>, C<sub>2</sub> and F<sub>2</sub>; Appendix Fig S2), suggesting that the treatment normalized the cerebral structure.

Nevertheless, the cerebral lactate levels, that are increased in *Coq9*<sup>R239X</sup> mice (Fig 2H<sub>2</sub>) compared to *Coq9*<sup>+/+</sup> mice (Fig 2G<sub>2</sub>), remained increased in *Coq9*<sup>R239X</sup> mice after the treatment (Fig 2I<sub>2</sub>).

In the skeletal muscle, the cytochrome c oxidase (COX) and succinate dehydrogenase (SDH) stainings showed an increase in type II fibers in *Coq9*<sup>R239X</sup> mice. After the treatment with  $\beta$ -RA, the proportion of type I and type II fibers was normalized (Fig EV2).

### Transcriptomics profile reveals a reduction in the neuroinflammatory genes

Next, we carried out an RNA-Seq experiment on brainstems from the three experimental mice groups, e.g., *Coq9*<sup>+/+</sup>, *Coq9*<sup>R239X</sup>, and *Coq9*<sup>R239X</sup> treated with  $\beta$ -RA. The over  $9 \times 10^9$  bases of the 101-bases sequencing reads aligned to 27,291 loci of the reference mouse genome. As Fig 3A shows, 298 genes were over-expressed in the *Coq9*<sup>R239X</sup> mice compared to the *Coq9*<sup>+/+</sup> mice, while 161 were under-expressed. On the other hand, 187 genes were over-expressed in the *Coq9*<sup>R239X</sup> mice compared to the *Coq9*<sup>R239X</sup> mice treated with  $\beta$ -RA, while 160 were under-expressed (Fig 3A). When comparing the pathways to which these differentially expressed genes belong, we observed a noticeably higher presence of genes belonging to inflammation signaling pathways in the *Coq9*<sup>R239X</sup> mice compared to the  $\beta$ -RA treated *Coq9*<sup>R239X</sup> or *Coq9*<sup>+/+</sup> mice (Fig 3B).

Of the 459 genes whose expression is significantly altered in *Coq9*<sup>R239X</sup> mice compared to *Coq9*<sup>+/+</sup>, 27 were significantly altered in *Coq9*<sup>R239X</sup> mice treated with  $\beta$ -RA compared to *Coq9*<sup>R239X</sup> mice. Interestingly, among these 27 genes, the ones that were over-expressed in *Coq9*<sup>R239X</sup> mice, compared to the *Coq9*<sup>+/+</sup> mice, became under-expressed in *Coq9*<sup>R239X</sup> mice treated with  $\beta$ -RA, compared to *Coq9*<sup>R239X</sup> mice, and *vice versa* (Fig 3C). Thus, the levels of these 27 genes were normalized. Most of these genes showed higher expression in *Coq9*<sup>R239X</sup> mice compared to *Coq9*<sup>+/+</sup> mice, and they mainly have inflammation and immune-related functions. For example, the inflammatory genes *Bgn* (biglycan), *Ccl6* (chemokine C-C motif ligand 6), *Cst7* (cystatin F), *Ifi2712a* (interferon, alpha-inducible protein 27 like 2A), *Ifitm3* (interferon-induced transmembrane protein 3), *Itgax* (integrin alpha X), and *Vav1* are up-regulated in *Coq9*<sup>R239X</sup> mice and normalized after the treatment.

### $\beta$ -RA does not directly act as anti-inflammatory agent

Because the transcriptomics profile uncovers a possible involvement of neuroinflammation in the therapeutic effect of  $\beta$ -RA, and since this molecule is an analogue of the anti-inflammatory salicylic acid, we tested whether  $\beta$ -RA may have a direct anti-inflammatory action. First, we incubated RAW cells with 1  $\mu$ g/ml LPS, which induces a NF- $\kappa$ B-mediated inflammatory response, as it is shown by the induction of iNOS (Fig 3D) and the release of IL-1 $\beta$ , IL-2, and TNF- $\alpha$  (Fig 3E). The pre-incubation with  $\beta$ -RA, however, did not modify the cellular iNOS expression (Fig 3D) or the cytokine levels in the cells supernatants (Fig 3E). Second, we quantified the cytokine levels in the brainstem of the three animals' experimental groups. The levels of IL-1 $\beta$ , IL-2, IFN- $\gamma$ , Gro- $\alpha$ , and TNF- $\alpha$  did not experience major changes (Fig 3F). Third, we tested whether  $\beta$ -RA may increase the survival in two models of neuroinflammation and early death due to mitochondrial Complex I deficiency, i.e., the zebrafish embryos treated with MPTP, which mimics Parkinson disease (Díaz-Casado *et al*, 2018); and the *Ndufs4* knockout mouse model, which mimics Leigh syndrome (Quintana *et al*, 2010). In both cases, the treatment with  $\beta$ -RA did not induce any change in the animal survival (Fig 3G and I) or the presence of malformations (Fig 3H). Because the inhibition of mTORC1 may mediate the anti-inflammatory actions of salicylates (Cameron *et al*, 2016), we also quantified the S6RP/S6R ratio as a marker of mTORC1 activity. Consistently with the other data, the  $\beta$ -RA did not modify the S6RP/S6R ratio in the brain (Appendix Fig S3A) and the kidneys (Appendix Fig S3B) of *Coq9*<sup>R239X</sup> mice treated with  $\beta$ -RA, suggesting that this molecule does not inhibit mTORC1 *in vivo*. Overall, these results do not support a direct role of  $\beta$ -RA in the repression of the typical neuroinflammatory pathways.

### $\beta$ -RA improves mitochondrial bioenergetics in peripheral tissues of *Coq9*<sup>R239X</sup> mice

The persistent lactate peak observed in the brain spectroscopy after the  $\beta$ -RA treatment suggests that the treatment does not have any effect on mitochondrial bioenergetics in the brain. To confirm this premise, we evaluated the mitochondrial function in the brain, but also in the kidneys, muscle, and heart (tissues clinically important in CoQ deficiency syndrome) of *Coq9*<sup>+/+</sup> mice, *Coq9*<sup>R239X</sup> mice, and *Coq9*<sup>R239X</sup> mice treated with  $\beta$ -RA.

In the brain of the mutant mice, the activities of the CoQ-dependent mitochondrial Complexes I+III (CI+III) and CII+III, the levels of sulfide:quinone oxidoreductase (SQOR), the assembly of C-III into the supercomplexes (SC), and the mitochondrial oxygen consumption rate (OCR) were significantly decreased (Fig 4A–E) compared to the values of wild-type animals. The  $\beta$ -RA treatment did not induce any change in those parameters in the brain of *Coq9*<sup>R239X</sup> mice (Fig 4A–E). In the kidneys of the mutant mice, the activity of the CI+III, the levels of SQOR, and the OCR were significantly decreased (Fig 4F–J), compared to the values of wild-type animals. These changes were not due to a potential capability of  $\beta$ -RA to act as an electron carrier in the mitochondrial respiratory chain because the CI+III activity did not change after adding 50  $\mu$ M  $\beta$ -RA into the reaction mix (Appendix Fig S4). The  $\beta$ -RA treatment partially

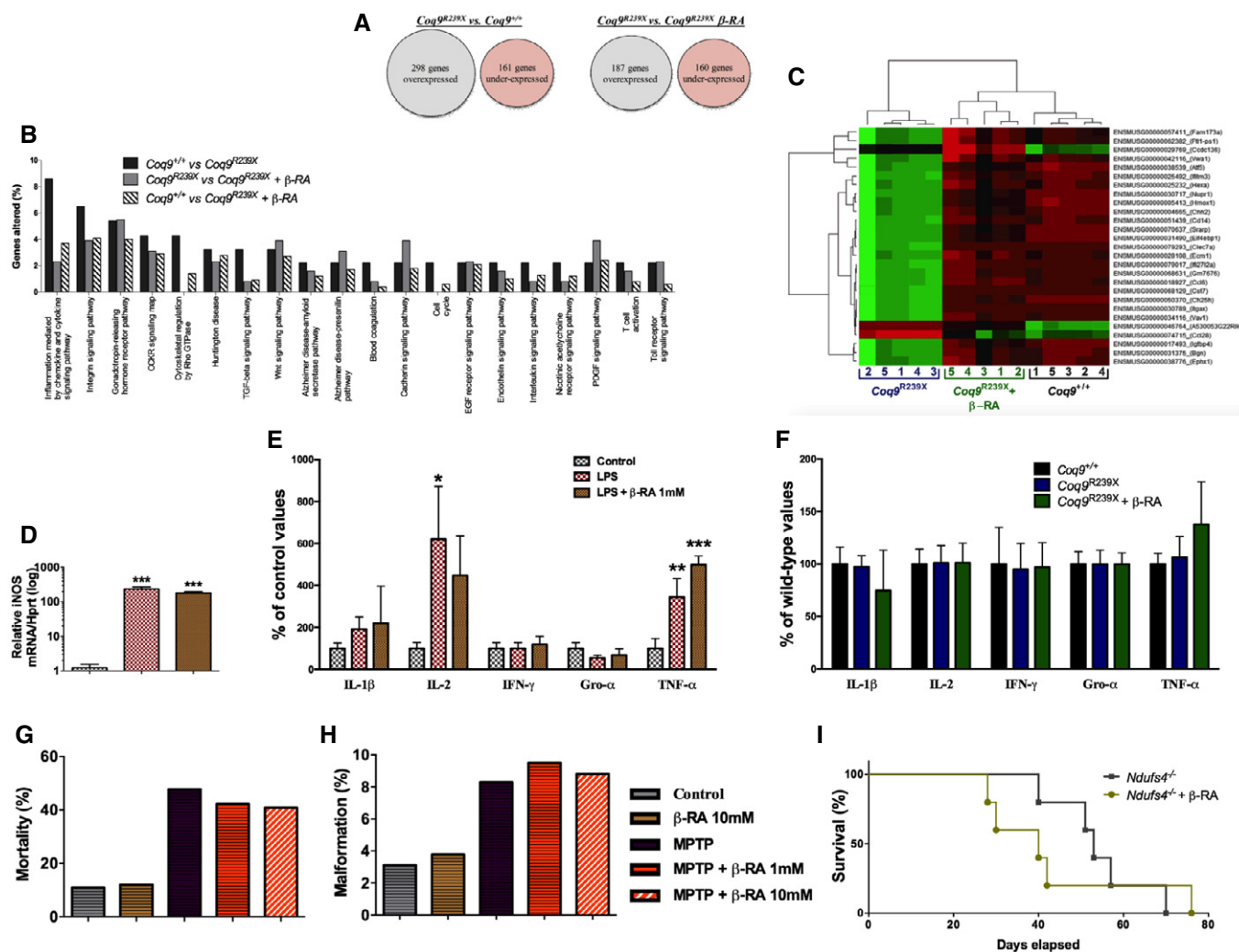


**Figure 3. Effect of the β-RA treatment on genes expression profiles and neuroinflammatory-related features.**

- A Global differences in the levels of gene expression between experimental groups.
- B Only pathways with more than one gene significantly altered in *Coq9<sup>R239X</sup>* compared to *Coq9<sup>+/+</sup>* mice are considered for this figure. The y-axis represents the percentage of genes corresponding to a pathway in the sample of genes whose expression level is significantly altered in a comparison between mice samples.
- C Heatmap showing the comparative landscape of the expression level per sample of the 27 genes whose expression was altered by the mutation and normalized by the β-RA treatment. The column numbers correspond to the different samples and the row names are gene codes composed of the ENSEMBL gene ID and the gene symbol (between parentheses). The green means comparatively higher, red means comparatively lower, and black means no difference in expression level ( $n = 5$  for each group).
- D iNOS expression levels in RAW cells after stimulation with LPS ( $n = 3$  for each group).
- E Cytokine levels in the culture supernatant of RAW cells after stimulation with LPS ( $n = 3$  for each group).
- F Cytokine levels in the brainstem of *Coq9<sup>+/+</sup>* mice, *Coq9<sup>R239X</sup>* mice, and *Coq9<sup>R239X</sup>* mice treated with β-RA ( $n = 7$  for each group).
- G, H Mortality rate (G) and (H) percentage of malformations in zebrafish embryos treated with MPT and the effect of β-RA treatment.
- I Survival curve of *Ndufs4* knockout mice and *Ndufs4* knockout mice treated with β-RA [Log-rank (Mantel-Cox) test;  $n = 5$  for each group; see Appendix Table S3 for exact *P*-values].

Data information: Data in panels (D–F) are expressed as mean  $\pm$  SD. \* $P < 0.05$ ; \*\* $P < 0.01$ ; \*\*\* $P < 0.001$ ; LPS or LPS + β-RA versus control. + $P < 0.05$ ; LPS or LPS + β-RA versus control (one-way ANOVA with a Tukey's *post hoc* test; see Appendix Table S3 for exact *P*-values).

normalized the CI+III activity and induced a significant increase of SQOR levels and the OCR (Fig 4F–J). On the contrary, assembly of C-I into the supercomplexes did not change in any experimental group (Appendix Fig S5). In the skeletal muscle of the mutant mice, the activity of the CI+III was significantly decreased, while the CII+III activity did not change (Fig 4K and L), compared to the values of wild-type animals. The β-RA treatment normalized the

CI+III activity (Fig 4K). In the heart of *Coq9<sup>R239X</sup>* mice, the activities of the CI+III and CII+III, as well as the levels of SQOR, were significantly decreased (Fig 4M–O), compared to the values of wild-type animals. Again, the β-RA treatment partially normalized the CI+III, CII+III activities, and the levels of SQOR, although partially in this case (Fig 4M–O). Therefore, these results illustrate tissue-specific responses to β-RA treatment in the mitochondrial bioenergetics.

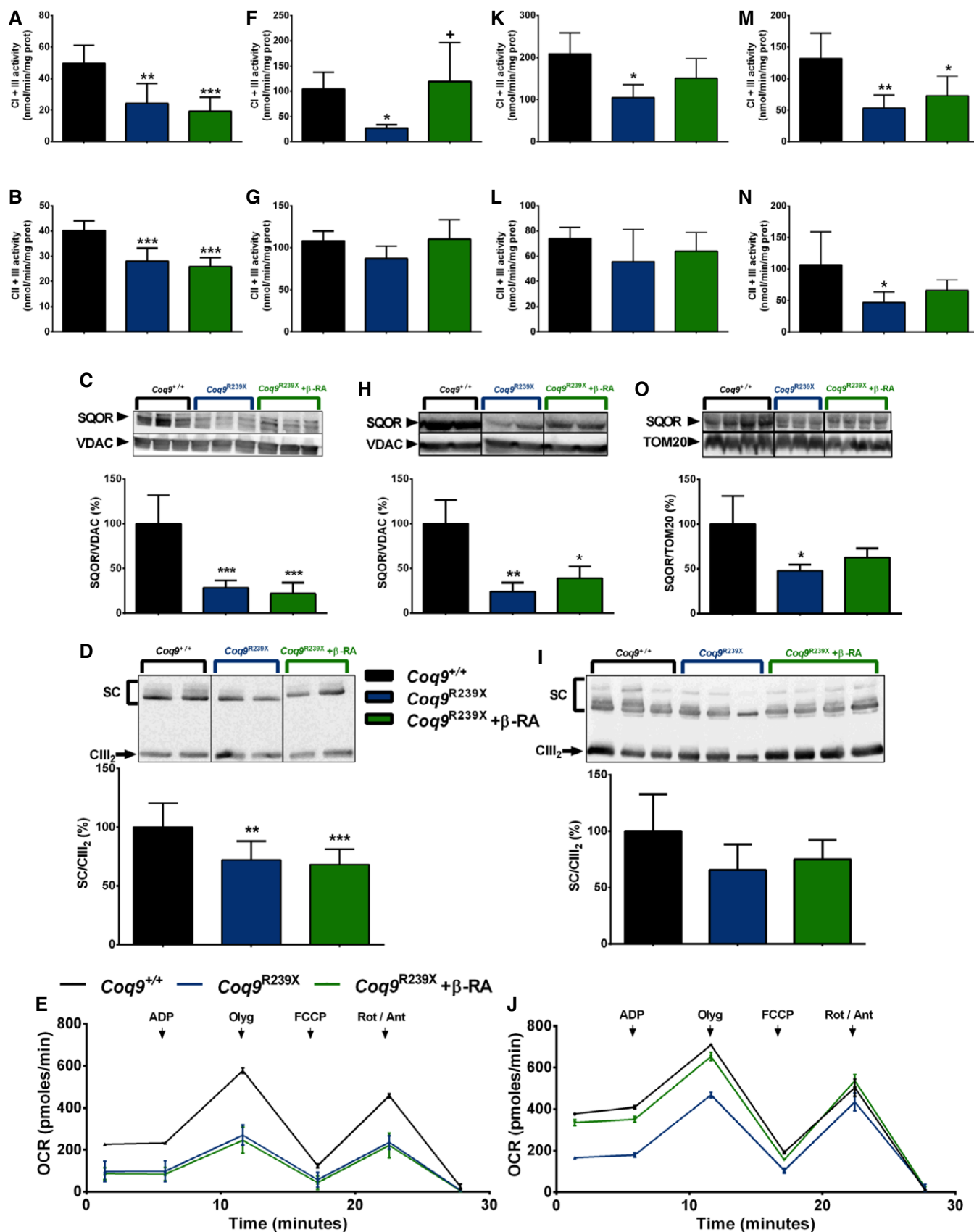


Figure 4.

**Figure 4. Tissue-specific differences in mitochondrial function after  $\beta$ -RA treatment in  $Coq9^{R239X}$  mice.**

A–O (A, F, K, M) CoQ-dependent Complex I+III activities in brain (A) and kidneys (F), skeletal muscle (K), and heart (M). (A):  $Coq9^{+/+}$ ,  $n = 5$ ;  $Coq9^{R239X}$ ,  $n = 6$ ;  $Coq9^{R239X}$  after  $\beta$ -RA treatment,  $n = 7$ . (F):  $Coq9^{+/+}$ ,  $n = 4$ ;  $Coq9^{R239X}$ ,  $n = 6$ ;  $Coq9^{R239X}$  after  $\beta$ -RA treatment,  $n = 4$ . (K):  $Coq9^{+/+}$ ,  $n = 3$ ;  $Coq9^{R239X}$ ,  $n = 6$ ;  $Coq9^{R239X}$  after  $\beta$ -RA treatment,  $n = 3$ . (M):  $Coq9^{+/+}$ ,  $n = 5$ ;  $Coq9^{R239X}$ ,  $n = 6$ ;  $Coq9^{R239X}$  after  $\beta$ -RA treatment,  $n = 6$ . (B, G, L, N) CoQ-dependent Complex II+III activities in brain (B) and kidneys (G), skeletal muscle (L) and heart (N). (B):  $Coq9^{+/+}$ ,  $n = 5$ ;  $Coq9^{R239X}$ ,  $n = 6$ ;  $Coq9^{R239X}$  after  $\beta$ -RA treatment,  $n = 7$ . (G):  $Coq9^{+/+}$ ,  $n = 5$ ;  $Coq9^{R239X}$ ,  $n = 6$ ;  $Coq9^{R239X}$  after  $\beta$ -RA treatment,  $n = 6$ . (L):  $Coq9^{+/+}$ ,  $n = 5$ ;  $Coq9^{R239X}$ ,  $n = 6$ ;  $Coq9^{R239X}$  after  $\beta$ -RA treatment,  $n = 7$ . (N):  $Coq9^{+/+}$ ,  $n = 6$ ;  $Coq9^{R239X}$ ,  $n = 6$ ;  $Coq9^{R239X}$  after  $\beta$ -RA treatment,  $n = 6$ . (C, H, O) Representative Western blot and quantitation of Western blot bands of SQOR in mitochondrial fractions of brain (C) and homogenates extracts from kidneys (H) and heart (O). (C):  $Coq9^{+/+}$ ,  $n = 6$ ;  $Coq9^{R239X}$ ,  $n = 6$ ;  $Coq9^{R239X}$  after  $\beta$ -RA treatment,  $n = 6$ . (H):  $Coq9^{+/+}$ ,  $n = 4$ ;  $Coq9^{R239X}$ ,  $n = 3$ ;  $Coq9^{R239X}$  after  $\beta$ -RA treatment,  $n = 3$ . (O):  $Coq9^{+/+}$ ,  $n = 4$ ;  $Coq9^{R239X}$ ,  $n = 3$ ;  $Coq9^{R239X}$  after  $\beta$ -RA treatment,  $n = 4$ . (D, I) Blue-native gel electrophoresis (BNGE) followed by C-III immunoblotting analysis of mitochondrial supercomplexes in brain (D) and kidneys (I). (D):  $Coq9^{+/+}$ ,  $n = 9$ ;  $Coq9^{R239X}$ ,  $n = 10$ ;  $Coq9^{R239X}$  after  $\beta$ -RA treatment,  $n = 11$ . (I):  $Coq9^{+/+}$ ,  $n = 5$ ;  $Coq9^{R239X}$ ,  $n = 6$ ;  $Coq9^{R239X}$  after  $\beta$ -RA treatment,  $n = 7$ . (E, J) Mitochondrial oxygen consumption rate (represented as State 3<sub>o</sub>, in the presence of ADP and substrates) in brain (E) and kidneys (J). The data represent three technical replicates and the figures are representative of three biological replicates.  $Coq9^{+/+}$  mice,  $Coq9^{R239X}$  mice, and  $Coq9^{R239X}$  mice after  $\beta$ -RA treatment were included in all graphs. Data are expressed as mean  $\pm$  SD. \* $P < 0.05$ ; \*\* $P < 0.01$ ; \*\*\* $P < 0.001$ ;  $Coq9^{R239X}$  or  $Coq9^{R239X}$  after  $\beta$ -RA treatment versus  $Coq9^{+/+}$ . \* $P < 0.05$ ;  $Coq9^{R239X}$  versus and  $Coq9^{R239X}$  after  $\beta$ -RA treatment (one-way ANOVA with a Tukey's *post hoc* test; see Appendix Table S4 for exact *P*-values).

Source data are available online for this figure.

### $\beta$ -RA reduces DMQ<sub>9</sub> in peripheral tissues of $Coq9^{R239X}$ mice

$Coq9^{R239X}$  mice present widespread deficiency of CoQ<sub>9</sub> (major CoQ form in rodents) and CoQ<sub>10</sub> (minor CoQ form in rodents). Because COQ9 protein is needed for the COQ7 hydroxylation reaction,  $Coq9^{R239X}$  mice also show accumulation of demethoxyubiquinone-9 (DMQ<sub>9</sub>), the substrate of COQ7 (Garcia-Corzo *et al.*, 2013). To test whether the general health improvement after  $\beta$ -RA treatment was due to the effects of this compound on CoQ biosynthesis, and to check whether the tissue-specific differences in mitochondrial bioenergetics were due to variances in the CoQ metabolism, we measured the levels of CoQ<sub>9</sub>, CoQ<sub>10</sub> and DMQ<sub>9</sub> in the most relevant tissues. As previously reported, the levels of CoQ<sub>9</sub> (Fig 5A, E, I, M and Q) and CoQ<sub>10</sub> (Fig 5B, F, J, N and R) were severely decreased in the brain (Fig 5A and B), kidneys (Fig 5E and F), liver (Fig 5I and J), skeletal muscle (Fig 5M and N), and heart (Fig 5Q and R) of  $Coq9^{R239X}$  mice. At the same time, the levels of DMQ<sub>9</sub> were significantly increased in the same tissues (Fig 5C, G, K, O and S) and, therefore, the DMQ<sub>9</sub>/CoQ<sub>9</sub> ratios were significantly increased (Fig 5D, H, L, P, and T) in  $Coq9^{R239X}$  mice. After the treatment with  $\beta$ -RA, the levels of CoQ<sub>9</sub> slightly increased only in the kidneys (Fig 5E), but not in the other tissues (Fig 5A, I, M, and Q) of the mutant mice. CoQ<sub>10</sub> also showed a trend toward increased levels in the kidneys of  $Coq9^{R239X}$  mice after  $\beta$ -RA treatment (Fig 5F), although in the other tissues the levels of CoQ<sub>10</sub> did not change after  $\beta$ -RA treatment (Fig 5B, J, N and R). Importantly, the levels of DMQ<sub>9</sub> and, consequently, the DMQ<sub>9</sub>/CoQ<sub>9</sub> ratios were significantly decreased in the kidneys (Fig 5G and H), liver (Fig 5K and L), skeletal muscle (Fig 5O and P), and heart (Fig 5S and T) of  $Coq9^{R239X}$  mice treated with  $\beta$ -RA, suggesting that  $\beta$ -RA exerts an influence in the CoQ biosynthetic pathway. In the brain, however, the  $\beta$ -RA treatment did not induce changes in the levels of DMQ<sub>9</sub> or DMQ<sub>9</sub>/CoQ<sub>9</sub> ratio (Fig 5C and D). Taken together, these results suggest that the improvement of mitochondrial bioenergetics occurs only in the tissues with decreased DMQ<sub>9</sub>/CoQ<sub>9</sub> ratio after the treatment.

To check whether the levels of CoQ<sub>9</sub> and DMQ<sub>9</sub> can be further modified during the time of the treatment or with a higher dose of  $\beta$ -RA, we also quantified the levels of both quinones in tissues of mice after 9 months of treatment or with the double dose of  $\beta$ -RA. The results showed that the levels of DMQ<sub>9</sub> levels and the DMQ<sub>9</sub>/CoQ<sub>9</sub> ratio were decreased in these two other experimental variants (Table EV1 and Appendix Figs S6 and S7). However, no

major differences were found in the results obtained under three experimental situations.

Because the tissue-specific differences observed in DMQ<sub>9</sub>/CoQ<sub>9</sub> ratio after  $\beta$ -RA treatment could be due to the bioavailability of this compound in the tissues after oral supplementation, we quantified the levels of  $\beta$ -RA in  $Coq9^{R239X}$  mice after oral supplementation and compared the data to those obtained after acute intraperitoneal (i.p.) administration. The compound was detected in all the examined tissues, including the brain, by both oral and i.p. administration (Table EV2 and Appendix Fig S8). The highest values of  $\beta$ -RA were found in plasma and kidneys, while the results in brain and liver were similar (Table EV2 and Appendix Fig S8). In the non-treated animals,  $\beta$ -RA was not detected, except in the kidney of one animal (Table EV2 and Appendix Fig S8). In order to see whether the effect observed after the treatment was due to  $\beta$ -RA and not to any other metabolite derived from it, we developed an UPLC-MS screening experiment. The other hydroxybenzoic acid detected in the samples was the 4-HB, but no statistic differences were found between the experimental groups (Appendix Table S1). Therefore, the bioavailability of  $\beta$ -RA does not completely explain the tissue-specific differences in CoQ metabolism since brain and liver showed similar levels of  $\beta$ -RA.

### The effect of $\beta$ -RA over CoQ biosynthetic pathway is mediated by a mild stabilization of the Complex Q

To try to understand the mechanism involved in the reduction in the levels of DMQ<sub>9</sub> observed after  $\beta$ -RA treatment, we quantified the levels of main CoQ biosynthetic proteins. The levels of PDSS2 and COQ2, which are not part of Complex Q, did not experience major changes in the brain (Appendix Fig S9A and B), kidneys (Appendix Fig S9C and D), and heart (Appendix Fig S9F and G) of the three experimental groups, and only a decrease in the COQ2 levels was appreciated in the kidneys of  $Coq9^{R239X}$  mice (Appendix Fig S9D). The levels of COQ4, COQ5, COQ6, COQ7, and COQ8A, which are components of the Complex Q, were consistently decreased in the brain (Fig 6A–E), kidneys (Fig 6F–J), and heart (Fig 6K–O) of  $Coq9^{R239X}$  mice compared to the same tissues in  $Coq9^{+/+}$  mice. Interestingly, the treatment with  $\beta$ -RA induced a trend toward increase on the levels of COQ4, COQ5, COQ6, and COQ8A in the kidneys (Fig 6F, G, H and J) and heart (Fig 6K, L, M and O), but not in the brain (Fig 6A, B, C and E). On the contrary,

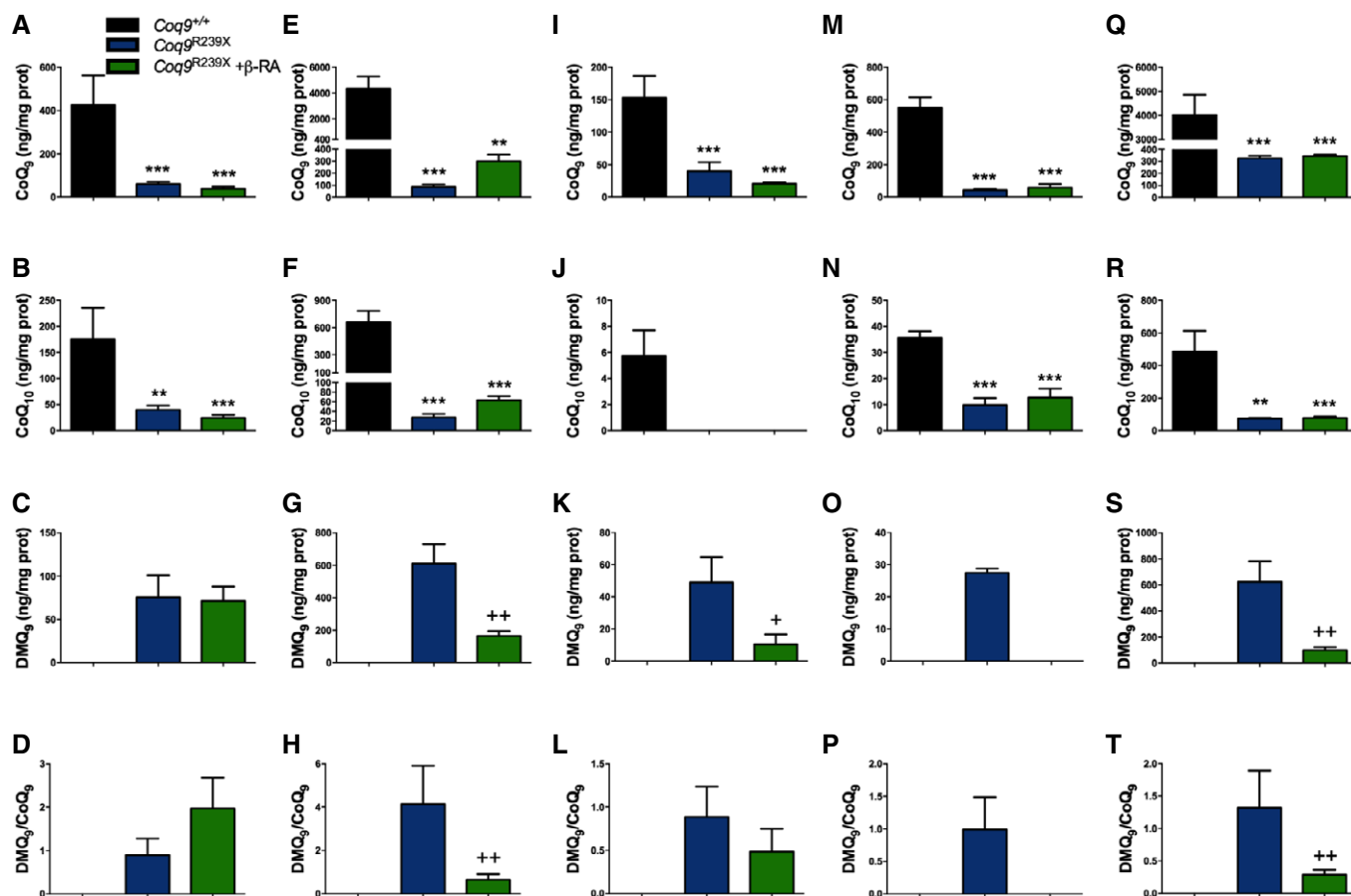


**Figure 5. Tissue-specific differences in the levels of CoQ<sub>9</sub>, CoQ<sub>10</sub>, and DMQ<sub>9</sub>, and in the DMQ<sub>9</sub>/CoQ<sub>9</sub> ratio after  $\beta$ -RA treatment in *Coq9<sup>R239X</sup>* mice.**

A–T Levels of CoQ<sub>9</sub> (A, E, I, M, Q), CoQ<sub>10</sub> (B, F, J, N, R), and DMQ<sub>9</sub> (C, G, K, O, S), as well as the DMQ<sub>9</sub>/CoQ<sub>9</sub> ratio (D, H, L, P, T) in brain (A–D), kidney (E–H), liver (I–L), skeletal muscle (M–P), and heart (Q–T) of *Coq9<sup>+/+</sup>* mice, *Coq9<sup>R239X</sup>* mice, and *Coq9<sup>R239X</sup>* mice after  $\beta$ -RA treatment. Data are expressed as mean  $\pm$  SD. \*\* $P$  < 0.01; \*\*\* $P$  < 0.001; *Coq9<sup>R239X</sup>* or *Coq9<sup>R239X</sup>* after  $\beta$ -RA treatment versus *Coq9<sup>+/+</sup>*. \* $P$  < 0.05; ++ $P$  < 0.01; *Coq9<sup>R239X</sup>* versus *Coq9<sup>R239X</sup>* after  $\beta$ -RA treatment (one-way ANOVA with a Tukey's *post hoc* test or *t*-test;  $n$  = 6 for each group; see Appendix Table S5 for exact *P*-values). Note that DMQ<sub>9</sub> was undetectable in tissues from *Coq9<sup>+/+</sup>* mice as well as in muscle of *Coq9<sup>R239X</sup>* mice treated with  $\beta$ -RA.

the levels of COQ7, which physically interacts with COQ9, were not modified by the  $\beta$ -RA treatment in any of the three tissues (Fig 6D, J and T). Overall, these results suggest that  $\beta$ -RA may induce the stabilization of the Complex Q, resulting in a decrease in the DMQ<sub>9</sub>/CoQ<sub>9</sub> ratio.

### The levels of DMQ<sub>9</sub> contribute to the disease phenotype

The results of the previous sections suggest that the DMQ<sub>9</sub>/CoQ<sub>9</sub> ratio is a key factor in the disease phenotype. To validate those results, we calculated the DMQ<sub>9</sub>/CoQ<sub>9</sub> ratio in the tissues of two additional experimental models: (i) the *Coq9<sup>Q95X</sup>* mouse model, which have widespread CoQ deficiency without compromising the lifespan (Luna-Sanchez *et al*, 2015); and (ii) the *Coq9<sup>R239X</sup>* mice treated with ubiquinol-10, which show an increase in the levels of CoQ<sub>10</sub> (Garcia-Corzo *et al*, 2014), resulting in an increase in the lifespan (Fig 1A); yet, this increased lifespan is not comparable to the one observed under  $\beta$ -RA treatment (Fig 1A). Our results show that, at 1 month of age, the DMQ<sub>9</sub>/CoQ<sub>9</sub> ratios in the tissues

of *Coq9<sup>Q95X</sup>* mice were significantly lower than in the tissues of *Coq9<sup>R239X</sup>* mice (Fig 7A and B; Appendix Fig S10). At 3 months of age, the DMQ<sub>9</sub> almost disappeared in the tissues of *Coq9<sup>Q95X</sup>*, but not in *Coq9<sup>R239X</sup>* mice (Fig 7C and D; Appendix Fig S10). In *Coq9<sup>R239X</sup>* mice, the treatment with ubiquinol-10 did not affect the levels of DMQ<sub>9</sub> and, therefore, the DMQ<sub>9</sub>/CoQ<sub>9</sub> ratios were still high in all tissues, while the CoQ<sub>10</sub> was increased (Fig 7E and F; Appendix Fig S11). Therefore, those results corroborate the correlation between DMQ<sub>9</sub>/CoQ<sub>9</sub> ratio and the severity of the disease phenotype.

### Steroid hormones or FGF21 do not mediate the tissues communication under CoQ deficiency

Because our data suggest that the modification of CoQ metabolism in peripheral tissues induces a reduction in the brain pathology in *Coq9<sup>R239X</sup>* mice treated with  $\beta$ -RA, we tried to identify a circulating signal molecule that may provide this tissue communication (e.g., kidney–brain, muscle–brain, heart–brain, or

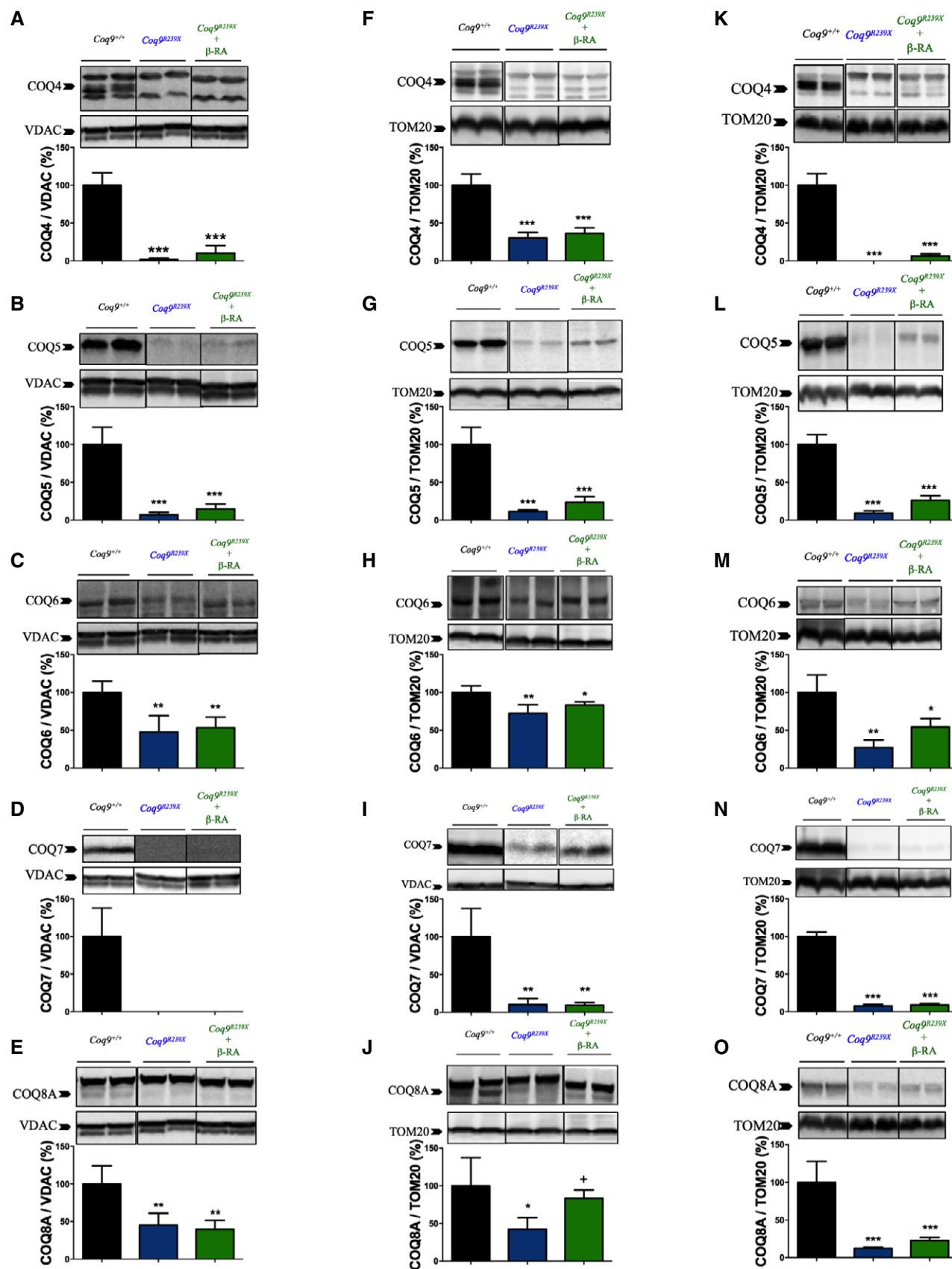


Figure 6.

**Figure 6. Effect of  $\beta$ -RA treatment in the tissue levels of CoQ biosynthetic proteins.**

A–O Representative images of Western blots of the CoQ biosynthetic proteins COQ4, COQ5, COQ6, COQ7, and COQ8A and the quantitation of the protein bands in the brain (A–E), kidneys (F–J), and heart (K–O) of *Coq9*<sup>+/+</sup>, *Coq9*<sup>R239X</sup>, and *Coq9*<sup>R239X</sup> mice treated with  $\beta$ -RA. *Coq9*<sup>+/+</sup> mice, *Coq9*<sup>R239X</sup> mice, and *Coq9*<sup>R239X</sup> mice after  $\beta$ -RA treatment were included in all graphs. Data are expressed as mean  $\pm$  SD. \* $P$  < 0.05; \*\* $P$  < 0.01; \*\*\* $P$  < 0.001; *Coq9*<sup>R239X</sup> or *Coq9*<sup>R239X</sup> after  $\beta$ -RA treatment versus *Coq9*<sup>+/+</sup>, \* $P$  < 0.05; *Coq9*<sup>R239X</sup> versus and *Coq9*<sup>R239X</sup> after  $\beta$ -RA treatment (one-way ANOVA with a Tukey's *post hoc* test;  $n$  = 5 for each group; see Appendix Table S6 for exact  $P$ -values).

Source data are available online for this figure.

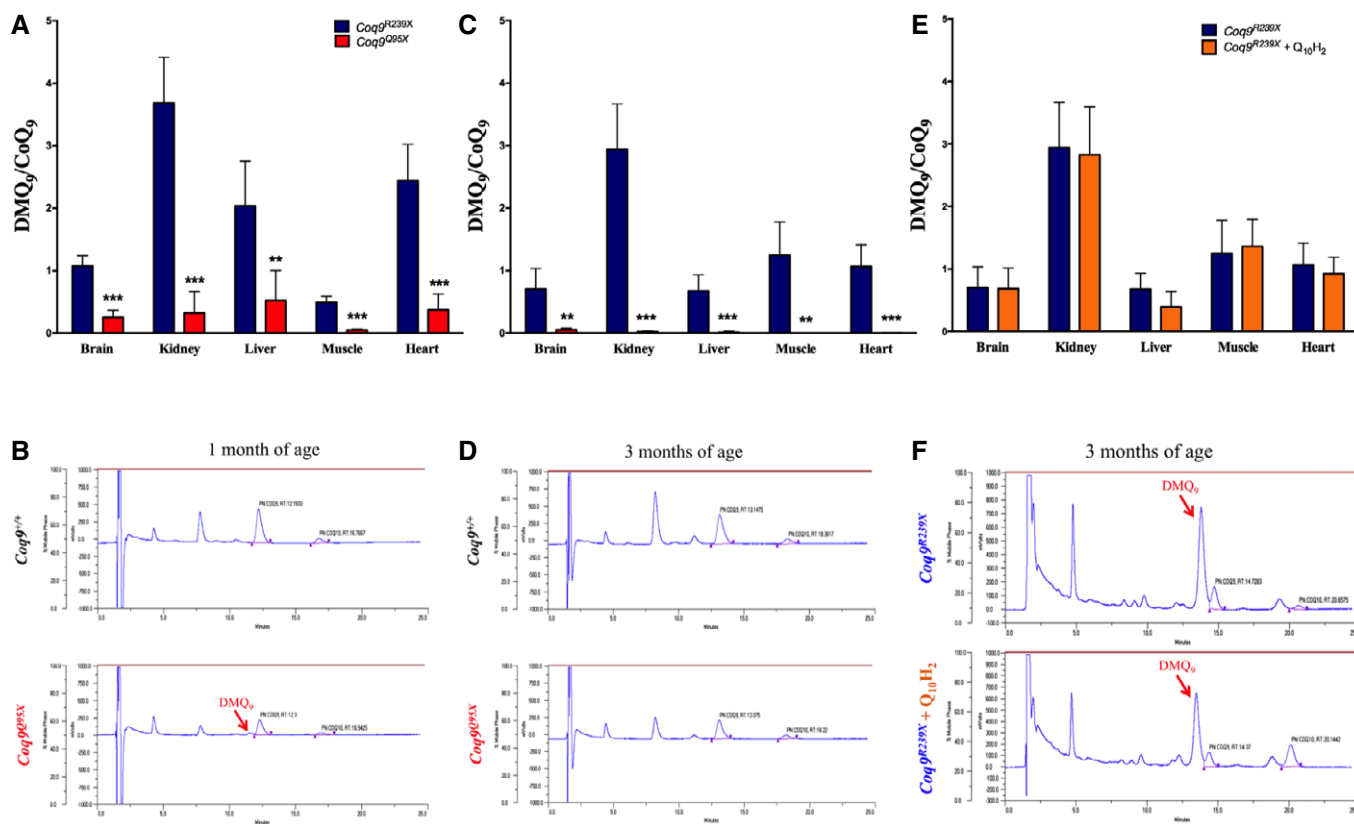
liver–brain). With that purpose, we quantified the steroid hormones, since some steps of their biosynthesis are localized in mitochondria; and FGF21, a recently identified biomarker for mitochondrial myopathies (Suomalainen *et al*, 2011). The results did not show any differences in the levels of corticosterone between the three experimental groups, both in males and females (Appendix Fig S12A and B). In male *Coq9*<sup>R239X</sup> mice, the levels of androstenedione and testosterone were significantly lower than those in male *Coq9*<sup>+/+</sup> mice (Appendix Fig S9C and D). After  $\beta$ -RA treatment, the levels of both hormones were still lower than those in control animals (Appendix Fig S12C and D).

The levels of FGF21 in the target organ, the brain, were similar in *Coq9*<sup>+/+</sup> and *Coq9*<sup>R239X</sup> mice, while a slight increase was detected in the precursor form in *Coq9*<sup>R239X</sup> mice treated with  $\beta$ -RA,

compared to *Coq9*<sup>R239X</sup> mice (Appendix Fig S12E). In the liver, the main secretory organ of FGF21, the levels of FGF21 (both the precursor and the mature form) were similar in the three experimental groups (Appendix Fig S12F).

## Discussion

The treatment of primary or secondary mitochondrial diseases is, in most cases, still limited to a palliative care. In this study, we identify a novel treatment for primary CoQ deficiency. The treatment is based on the administration of  $\beta$ -RA, which reduces the molecular, histopathologic, and clinical signs of mitochondrial encephalopathy in a mouse model of encephalopathy associated with CoQ

**Figure 7. DMQ<sub>9</sub>/CoQ<sub>9</sub> ratio in other experimental conditions.**

A–F (A) DMQ<sub>9</sub>/CoQ<sub>9</sub> ratio in tissues from *Coq9*<sup>R239X</sup> and *Coq9*<sup>Q95X</sup> mice at 1 month of age. (C) DMQ<sub>9</sub>/CoQ<sub>9</sub> ratio in tissues from *Coq9*<sup>R239X</sup> and *Coq9*<sup>Q95X</sup> mice at 3 months of age. (E) DMQ<sub>9</sub>/CoQ<sub>9</sub> ratio in tissues from *Coq9*<sup>R239X</sup> mice and *Coq9*<sup>R239X</sup> mice treated with ubiquinol-10 during 2 months. (B, D, F) Representative chromatograms showing the different quinones in the kidneys. Data in panels (A, C, E) are expressed as mean  $\pm$  SD. \*\* $P$  < 0.01; \*\*\* $P$  < 0.001; *Coq9*<sup>Q95X</sup> versus *Coq9*<sup>R239X</sup> (t-test;  $n$  = 5 for each group; see Appendix Table S7 for exact  $P$ -values).

deficiency. The remarkable increase of survival after  $\beta$ -RA treatment was superior to that observed after ubiquinol-10 treatment, and the therapeutic effect was succeeded even if the treatment started in a symptomatic period. The striking increase in animal survival and the general health improvement after the  $\beta$ -RA treatment was achieved even though the levels of CoQ and mitochondrial function were not increased in the brain, which is the most relevant tissue for the development of the disease. In peripheral tissues, however,  $\beta$ -RA induced a decrease in the DMQ<sub>9</sub>/CoQ<sub>9</sub> ratio, resulting in a bioenergetics improvement that may exert a key influence on the brain pathology. Accordingly, we provide additional data about the DMQ<sub>9</sub>/CoQ<sub>9</sub> ratio in the *Coq9*<sup>Q95X</sup> mouse model and in *Coq9*<sup>R239X</sup> mice treated with ubiquinol-10, and both cases support the importance of the DMQ<sub>9</sub>/CoQ<sub>9</sub> ratio in the progression of the clinical symptoms associated with CoQ deficiency syndrome.

The initial hypothesis for this study was that  $\beta$ -RA could be used in the CoQ biosynthetic pathway and bypasses the defect in COQ9-COQ7, increasing the endogenous levels of CoQ (Luna-Sanchez *et al*, 2015; Pierrel, 2017). However, our results show that the bypass effect would be limited because only the kidneys, the tissue with higher levels of  $\beta$ -RA, showed a moderate increase in the levels of CoQ in the mutant mice after the treatment. Nevertheless, the levels of DMQ<sub>9</sub> were significantly decreased not only in the kidneys but also in the skeletal muscle, liver, and heart. Those results hint that the CoQ biosynthetic pathway might use  $\beta$ -RA as a substrate whose Km is probably higher than the natural substrate, 4-HB, and for that reason the reduction of the DMQ<sub>9</sub> levels is not accompanied by an increase of CoQ<sub>9</sub> in tissues where the  $\beta$ -RA does not reach a threshold (Pierrel, 2017). Also, the stabilization of the Complex Q may contribute to this effect, since the levels of COQ4, COQ5, COQ6, and COQ8A were slightly increased in the kidneys and heart after  $\beta$ -RA treatment. Consistent with those results, 4-HB or vanillic acid induced an increase of the CoQ biosynthetic protein *in vitro* (Herebian *et al*, 2017b,c). Moreover, we must also consider that the  $\beta$ -RA administration was able to increase the levels of CoQ<sub>9</sub> in renal and cardiac mitochondria, as well as in muscle tissue in a conditional *Coq7* KO model, which lacks COQ7 protein (Wang *et al*, 2015, 2017). Nevertheless, the cerebral CoQ<sub>9</sub> levels after  $\beta$ -RA supplementation were not determined in the conditional *Coq7* KO mice (Wang *et al*, 2015, 2017). Because *Coq9*<sup>R239X</sup> mice has reduced levels not only of COQ7 but also of COQ4, COQ5, COQ6, and COQ8A (Luna-Sanchez *et al*, 2015), it is also possible that the limitation of the  $\beta$ -RA to generally increase the CoQ<sub>9</sub> levels in *Coq9*<sup>R239X</sup> mice could be due to the disruption of the Complex Q observed in this mouse model. The combination of both arguments could explain the lack of effect over the CoQ biosynthesis pathway in the brain. In either case, our data on the *Coq9*<sup>R239X</sup> mouse model together with those obtained in the *Coq7* conditional KO model indicate that it is possible to influence the CoQ biosynthesis *in vivo* with the use of the appropriated 4-HB analog(s). These results partially corroborate previous data *in vitro* using mutant yeasts and human skin fibroblasts derived from patients with primary CoQ deficiency (Ozeir *et al*, 2011; Xie *et al*, 2012; Doimo *et al*, 2014; Freyer *et al*, 2015; Luna-Sanchez *et al*, 2015; Herebian *et al*, 2017b,c; Pierrel, 2017; Wang *et al*, 2017).

While the levels of CoQ<sub>9</sub> and CoQ<sub>10</sub> were doubled in the kidneys of *Coq9*<sup>R239X</sup> mice after the treatment, the levels reached after the treatment were barely 5% of the wild-type levels. The reduction in

the DMQ<sub>9</sub> levels after the therapy, and as a consequence, the DMQ<sub>9</sub>/CoQ<sub>9</sub> ratio, was more important in terms of absolute values, as well as more consistent because the response was similar in all peripheral tissues. Importantly, the decrease in DMQ<sub>9</sub>/CoQ<sub>9</sub> ratio in peripheral tissues (like kidneys, heart, and muscle) was enough to increase the CoQ-dependent complexes activities up to normalizing the mitochondrial respiration. Therefore, the effect of the  $\beta$ -RA treatment in the function of the renal, muscular, and cardiac mitochondria must be due to the reduction of the DMQ<sub>9</sub>/CoQ<sub>9</sub> ratio. While DMQ is not commercial available to develop more direct experiments, Yang *et al* (2011) were able to exchange the quinone pools between the mitochondria from wild-type and Clk-1 (= *Coq7*) mutated worms, demonstrating that DMQ<sub>9</sub> was the responsible of the inhibition of the electron transfer from complex I to ubiquinone in the mitochondrial respiratory chain, probably due to the competition of CoQ and DMQ for the same binding site, together with the inability of DMQ to transfer electrons (Arroyo *et al*, 2006). Our results in mice suggest that DMQ could also inhibit the electron transfer from complex II to ubiquinone, a fact that was not observed in worms (Yang *et al*, 2011). Those differences may reflect the diverse structure and functionality of the mitochondria in different organisms, tissues, and cell types (Vafai & Mootha, 2012). Thus, our study points out the importance of the DMQ<sub>9</sub>/CoQ<sub>9</sub> ratio in the disease phenotype, a fact that is further supported by several evidences: (i) The *Coq9*<sup>Q95X</sup> mouse model has low levels of DMQ<sub>9</sub> and higher levels of CoQ biosynthetic proteins (compared to the *Coq9*<sup>R239X</sup> mouse model), and the lifespan is not compromised; (ii) the treatment with ubiquinol-10 in *Coq9*<sup>R239X</sup> mice does not change the DMQ<sub>9</sub> levels and its therapeutic effects are significantly lower than those after  $\beta$ -RA treatment; (iii) the reduction in the DMQ<sub>9</sub> levels in the *Coq7* conditional KO mice after  $\beta$ -RA therapy may also contribute to the increased survival observed in this mouse model, although the phenotype of this mouse model is not clear (Wang *et al*, 2015); and (iv) patients with high levels of DMQ<sub>10</sub> in the samples used for the diagnostic (muscle and/or skin fibroblasts) are associated to severe clinical presentations (Duncan *et al*, 2009; Freyer *et al*, 2015; Danhauser *et al*, 2016; Wang *et al*, 2017; Smith *et al*, 2018).

Because the levels of CoQ<sub>9</sub> and DMQ<sub>9</sub> did not change in the brain of the *Coq9*<sup>R239X</sup> mice after the treatment, this tissue did not experience any improvement in the mitochondrial function after  $\beta$ -RA therapy. However, even if the treatment does not have any detectable effect at the cerebral mitochondria, the *Coq9*<sup>R239X</sup> mice showed a clear and profound reduction in the spongiform degeneration, reactive astrogliosis, and oxidative damage, leading to an absence of brain injuries after the  $\beta$ -RA therapy. Those effects are, therefore, independent of the CoQ<sub>9</sub> and DMQ<sub>9</sub> levels in the brain. Thus, two complementary hypotheses could explain the therapeutic effects of  $\beta$ -RA in the brain of *Coq9*<sup>R239X</sup> mice. First,  $\beta$ -RA may have CoQ-independent functions with therapeutic potential for mitochondrial encephalopathies. The transcriptomics data showing a decrease in the expression levels of some inflammatory genes, and the fact that  $\beta$ -RA is a structural analogue of salicylic acid (Gomez-Guzman *et al*, 2014), would support this hypothesis. However, our experimental data do not support this hypothesis because: (i) The microglia distribution and the cytokines levels did not experience major changes between *Coq9*<sup>R239X</sup> mice and *Coq9*<sup>R239X</sup> mice treated with  $\beta$ -RA; (ii)  $\beta$ -RA did not reduce iNOS expression or cytokines release in RAW

cells stimulated with LPS; (iii)  $\beta$ -RA did not have therapeutic effects in pharmacological or genetic models of neuroinflammation, e.g., the MPTP-induced zebrafish model of Parkinson disease and the *Ndufs4* mouse model of Leigh syndrome; and (iv)  $\beta$ -RA did not inhibit mTORC1 *in vivo*. Thus, the changes in the expression levels of some inflammatory genes may reflect the reduction in the astrogliosis. In fact, some genes associated with chemokine (e.g., C-C Motif Chemokine Ligands family) and cytokine signaling (e.g., *Cd14*, *Ifitm3*, *Hmox1*), immune response (*Nurp1*), cell cycle (e.g., *Eif4bpb1*), cell adhesion (e.g., *Ecm1*, *Igfb4*), and lipid metabolism (e.g., *Ch25*) have been also associated to reactive astrogliosis (Zamanian et al, 2012; Colombo & Farina, 2016) and, therefore, the reduction observed in these genes could be due to the reduction in the astrogliosis. Our data also suggest that, similarly to other mitochondrial encephalopathies (Lax et al, 2012; Tegelberg et al, 2017), the neuroinflammation associated with microglia activation is not an important factor in the mitochondrial encephalopathy associated with CoQ deficiency.

The second hypothesis is that the reduction in DMQ<sub>9</sub>/CoQ<sub>9</sub> ratio in peripheral tissues and the subsequent improvement of mitochondrial bioenergetics may provide some tissue–brain cross-talk in order to reduce the astrogliosis, spongiosis, and its associated brain injury. While we were not able to reveal how the peripheral tissues communicate with the brain in this situation, a recent study about gene therapy in a mouse model of Leigh syndrome also suggests that the correction of the gene defect in peripheral tissues is important to reduce brain pathology (Di Meo et al, 2017). The studies about the kidney–brain, heart–brain, or liver–brain cross-talk, as well as the presence of a gut–brain axis, would support the concept of an influence of peripheral tissues in the brain pathology, and reactive astrogliosis in particular (Mayo et al, 2014; Butterworth, 2015; Rothhammer et al, 2016, 2017; Miranda et al, 2017; Thackeray et al, 2018).

In conclusion, our study shows that  $\beta$ -RA is a powerful therapeutic agent for the mitochondrial encephalopathy due to CoQ deficiency, a disease that is increasingly diagnosed with exome sequencing, with an estimation of more the 120,000 cases worldwide (Hughes et al, 2017). The therapeutic results are greater than those obtained by the classical oral CoQ supplementation because of the decrease of the DMQ/CoQ ratio. Therefore,  $\beta$ -RA should be preferentially considered for the treatment of human CoQ<sub>10</sub> deficiency with accumulation of DMQ<sub>10</sub>, as it has been reported in patients with mutations in *COQ9*, *COQ7*, or *COQ4* (Duncan et al, 2009; Freyer et al, 2015; Danhauser et al, 2016; Herebian et al, 2017b; Wang et al, 2017; Smith et al, 2018) but also in cells under siRNA knockdown of *COQ3*, *COQ5* and *COQ6* (Herebian et al, 2017b). Similar principles could be applied for 3,4-hydroxybenzoic acid, vanillic acid, 2-methyl-4-hydroxybenzoic acid, or 2,3-dimethoxy-4-hydroxybenzoic acid in the cases of mutations in *COQ6*, *COQ5*, or *COQ3* (Heeringa et al, 2011; Yoo et al, 2012; Ribas et al, 2014; Gigante et al, 2017; Herebian et al, 2017a; Pierrel, 2017), respectively. Furthermore, 4-HB analogs may provide therapeutic effects in other conditions, e.g., mitochondrial disorders, since secondary CoQ deficiency due to decreased levels of CoQ biosynthetic proteins have been recently reported in various mouse models of mitochondrial diseases (Kuhl et al, 2017); or metabolic diseases due to insulin resistance since secondary CoQ deficiency due to decreased levels of CoQ biosynthetic proteins have been recently described in

*in vitro* insulin resistance models and adipose tissue from insulin-resistant humans (Fazakerley et al, 2018). To apply the  $\beta$ -RA treatment into the clinic, the safety and dose–response studies included in a clinical trial should be first developed. Nevertheless,  $\beta$ -RA is a natural compound that is used as a flavor by the food industry (Adams et al, 2005), and its administration in wild-type mice at high doses does not have detrimental effects on the survival (Wang et al, 2015). Therefore, the safety study has a good prognosis and would allow the use of this compound at least as a compassionate option in cases of severe CoQ deficiencies due to mutations in *COQ9* or *COQ7*.

## Materials and Methods

### Experimental design

*Coq9*<sup>+/+</sup>, *Coq9*<sup>R239X</sup>, *Ndufs4*<sup>+/+</sup>, and *Ndufs4*<sup>-/-</sup> mice were used in the study. All mice have a mix of C57BL/6N and C57BL/6J genetic background. Mice were housed in the Animal Facility of the University of Granada under an SPF zone with lights on at 7:00 AM and off at 7:00 PM. Mice had unlimited access to water and rodent chow. The *Coq9*<sup>R239X</sup> mouse model (<http://www.informatics.jax.org/allele/key/829271>) was previously generated and characterized (Garcia-Corzo et al, 2013).  $\beta$ -RA was incorporated in the chow at a concentration of 1%, which provides a dose similar to the one (1 g/kg b.w./day) that was therapeutically successful in the *Coq7* conditional KO model (Wang et al, 2015). For a particular experiment, we doubled the dose by adding  $\beta$ -RA into the drinking water at a concentration of 0.5%, neutralizing the water with sodium bicarbonate. Also, a pilot survival study was done with  $\beta$ -RA in *Ndufs4* knockout mice, which show microgliosis and neuroinflammation (Quintana et al, 2010).

The motor coordination was evaluated by rotarod test at different months of age. Systolic blood pressure (SBP) and heart rate (HR) were measured in conscious, prewarmed, and restrained mice by tail-cuff plethysmography (Digital Pressure Meter LE 5001, Letica S.A., Barcelona, Spain) as described previously (Gomez-Guzman et al, 2014; Luna-Sanchez et al, 2017).

The therapeutic potential of  $\beta$ -RA was also assessed in zebrafish embryos treated with the neurotoxin 1-methyl-4-phenyl-1,2,3,6-tetrahydropyridine (MPTP), which is used to induce key features of Parkinson disease, including CI inhibition and neuroinflammation (Diaz-Casado et al, 2018). The embryos were exposed to MPTP from 24 hpf to 72 hpf, and  $\beta$ -RA was added to the wells from 72 hpf to 120 hpf. After completing the experiment protocol, at 120 hpf, the mortality rate was calculated as the percentage of dead embryos with respect to total embryos. Edema, the most common malformations, as well as tail and yolk abnormalities, were macroscopically quantified (Diaz-Casado et al, 2018). Adult zebrafish (*Danio rerio*) of the AB line were provided by ZFBiolabs S.L (Madrid, Spain) and used as breeding stocks. The fish line was maintained in the University of Granada's facility at a water temperature of 28.5 ± 1°C and under a photoperiod of 14:10 h (lights on at 08:00 h) in a recirculation aquaculture system (Aquaneering Incorporated, Barcelona, Spain).

Experiments in mice were performed according to a protocol approved by the Institutional Animal Care and Use Committee of

the University of Granada (procedures 9-CEEA-OH-2013) and were in accordance with the European Convention for the Protection of Vertebrate Animals used for Experimental and Other Scientific Purposes (CETS # 123) and the Spanish law (R.D. 53/2013). Experiments in zebrafish were performed according to a protocol approved by the Institutional Animal Care and Use Committee of the University of Granada (procedures CEEA 2010-275).

### Histology and immunohistochemistry

Multiple brain sections (4  $\mu$ m thickness) were deparaffinized with xylene and stained with hematoxylin and eosin (H&E). Immunohistochemistry was carried out in the same sections, using the following primary antibodies: anti-GFAP (Millipore, MAB360, dilution 1:400) and anti-Iba-1 (Wako, 019-19741, dilution 1:500). The detection of carbonyl groups as a marker of protein oxidation was performed using a commercial kit (OxyIHC™ Oxidative Stress Detection Kit; S7450, Millipore; Garcia-Corzo *et al*, 2013).

Type I and type II skeletal muscle fibers were examined through histochemical detection of cytochrome oxidase (COX) and succinate dehydrogenase (SDH) enzymes activity (Tanji & Bonilla, 2008).

### In vivo MRI and proton MRS

Magnetic resonance imaging and MRS studies were conducted using a 7 T horizontal bore magnet Bruker Biospec TM 70/20 USR designed for small animal experimentation. Following localizer scans, high-resolution axial and coronal T2-weighted datasets were acquired in order to visualize any cerebral or structural atrophy and to investigate for potential focal pathologies (Diaz *et al*, 2012).

### Transcriptome analysis by RNA-Seq

The RNeasy Lipid Tissue Mini Kit (Qiagen) was used to extract total RNAs from the brainstem of five animals in each experimental group. The RNAs were precipitated and their quality and quantity assessed using an Agilent Bioanalyzer 2100 and an RNA 6000 chip (Agilent Technologies). The cDNA libraries were then constructed using the TruSeq RNA Sample Prep Kit v2 (Illumina, Inc.) and their quality checked using an Agilent Bioanalyzer 2100 and a DNA 1000 chip (Agilent Technologies). The libraries were Paired End sequenced in a HiSeq 4000 system (Illumina, Inc.). We aimed for 4–5 Giga Bases outcome per sample. The quality of the resulting sequencing reads was assessed using FastQC. The GRCm38.p5 fasta and gtf files of the reference mouse genome were downloaded from the Ensembl database and indexed using the bwtsv option of BWA (Linden *et al*, 2012). BWA, combined with *xa2multi.pl* and SAMtools (Li *et al*, 2009), was also used for aligning the sequencing reads against the reference genome, and HTSeq was used for counting the number of reads aligned to each genomic locus (Mishanina *et al*, 2015). The alignments and counting were carried out in our local server following the protocols as described (Brzywczy *et al*, 2002; Di Meo *et al*, 2011).

After elimination of the genomic loci that aligned to < 5 reads in < 5 samples and normalization of the read counts by library size, the differential gene expression was detected using the Generalized Linear Model (glmLRT option) statistic in EdgeR (Hine *et al*, 2015). We used a 0.05 *P*-level threshold after False Discovery Rate

correction for type I error. The heatmap figure was made using the heatmap function in R (<https://www.r-project.org/>). Annotation of the differentially expressed genes was obtained from the Mouse Genome Informatics (<http://www.informatics.jax.org/>).

### Mitochondrial respiration

To isolate fresh mitochondria, mice were sacrificed and the organs were immediately extracted and placed in ice. The final crude mitochondrial pellet was re-suspended in MAS 1X medium (Luna-Sanchez *et al*, 2015). Mitochondrial respiration was measured by using an XFe<sup>24</sup> Extracellular Flux Analyzer (Seahorse Bioscience; Rogers *et al*, 2011). Respiration by the mitochondria was sequentially measured in a coupled state with the substrates (succinate, malate, glutamate, and pyruvate) present (basal respiration or State 2), followed by State 3o (phosphorylating respiration, in the presence of ADP and substrates); State 4 (non-phosphorylating or resting respiration) was measured after addition of oligomycin when all ADP was consumed, and then maximal uncoupler-stimulated respiration (State 3u; Luna-Sanchez *et al*, 2015). All data were expressed in pmol/min/mg protein.

### CoQ-dependent respiratory chain activities

Coenzyme Q-dependent respiratory chain activities were measured in submitochondrial particles, as previously described (Garcia-Corzo *et al*, 2014). To test whether  $\beta$ -RA works as a CoQ substitute in the mitochondrial respiratory chain, we also measure the CI-III activity after adding 50  $\mu$ M  $\beta$ -RA into the reaction mix. The results were expressed in nmol reduced cyt c/min/mg prot.

### Evaluation of supercomplexes formation by BNGE

Blue native gel electrophoresis (BNGE) was performed on crude mitochondrial fractions from mice kidneys and brain. Mitochondria were isolated and analyzed by BNGE, as previously described (Fernandez-Vizarra *et al*, 2002). After electrophoresis, the complexes were electroblotted onto PVDF membranes and sequentially tested with specific antibodies against CI, anti-NDUFA9 (Abcam, ab14713, dilution 1:5,000), CIII, anti-ubiquinol-cytochrome c reductase core protein I (Abcam, ab110252, dilution 1:5,000), and VDAC1 (Abcam, ab14734, dilution 1:5,000).

### Sample preparation and Western blot analysis in tissues

For Western blot analyses in mouse tissues, samples were homogenized and sonicated in T-PER<sup>®</sup> buffer (Thermo Scientific) with protease inhibitor cocktail (Pierce). For Western blot analyses in brain mitochondria, the pellets containing the mitochondrial fraction were re-suspended in RIPA buffer with protease inhibitor cocktail. Protein band intensity was normalized to VDAC1 (mitochondrial proteins), and the data were expressed in terms of percent relative to wild-type mice or control cells (Luna-Sanchez *et al*, 2015, 2017). The following primary antibodies were used: anti-SQRDL (Proteintech, 17256-1-AP, dilution 1:500), anti-PDSS2 (Proteintech, 13544-1-AP, dilution 1:500), anti-COQ2 (Origene, TA341982, dilution 1:2,500), anti-COQ4 (Proteintech, 16654-1-AP, dilution 1:2,000), anti-COQ5

**The paper explained****Problem**

CoQ<sub>10</sub> deficiency is a mitochondrial syndrome with heterogeneous clinical presentations. Typically, the patients with neurological symptoms or the cases with multisystemic affection respond poorly to the high doses of exogenous CoQ<sub>10</sub> supplementation due to the limitation of this molecule to cross the blood–brain barrier. Therefore, an alternative therapeutic option is needed for these patients.

**Results**

In this study, we have used a mouse model of mitochondrial encephalopathy due to CoQ deficiency to test a novel therapy based in the administration of  $\beta$ -resorcylic acid ( $\beta$ -RA), an analog of 4-hydroxybenzoic acid (4-HB), the precursor of the endogenous CoQ biosynthesis. In peripheral tissues, the  $\beta$ -RA was able to reduce the levels of demethoxyubiquinone, a CoQ biosynthetic intermediate metabolite that is toxic for the mitochondrial respiratory chain. Consequently, the mitochondrial bioenergetics performance was improved in peripheral tissues during  $\beta$ -RA treatment, leading to a reduction in the spongiosis and astrogliosis in the brain. As a result, the mutant mice treated with  $\beta$ -RA reached a maximum lifespan of 25 months of age, with a median survival of 22 months of age. This represents a significant increase in the animal survival if we compare the data to those of the untreated mutant mice, which reached a maximum age of 7 months, with a median survival of 5 months of age; or with the CoQ<sub>10</sub>-treated (in its reduced form, ubiquinol-10) mutant mice, which reached a maximum age of 17 months, with a median survival of 13 months of age.

**Impact**

The results support the use of  $\beta$ -RA at least as a compassionate option in cases of severe CoQ deficiencies due to mutations in *COQ9* or *COQ7*. Therefore, these findings deserve additional in depth research in order to translate the use of  $\beta$ -RA and/or other 4-HB analogs into the clinical practice.

(Proteintech, 17453-1-AP, dilution 1:1,000), anti-COQ6 (Proteintech, 12481-1-AP, dilution 1:500), anti-COQ7 (Proteintech, 15083-1-AP, dilution 1:1,000), anti-COQ8A (Proteintech, 15528-1-AP, dilution 1:2,500), anti-S6R (Cell Signaling, 2217, dilution 1:1,000), anti-S6RP (Cell Signaling, 2211, dilution 1:1,000), anti-FGF21 (Abcam, ab171941, dilution 1:1,000), anti-VDAC1 (Abcam, ab14734, dilution 1:5,000), anti-TOM20 (Proteintech, 11802-1-AP, dilution 1:5,000), and anti-GAPDH (Santacruz, sc-166574, dilution 1:200).

**Quantification of CoQ<sub>9</sub> and CoQ<sub>10</sub> levels in mice tissues**

CoQ<sub>9</sub> and CoQ<sub>10</sub> levels were determined via reversed-phase HPLC coupled to electrochemical (EC) detection (Lopez *et al*, 2010; Garcia-Corzo *et al*, 2013). The results were expressed in ng CoQ/mg prot.

**Quantification of  $\beta$ -RA levels and screening of potential derivate molecules in mice tissues**

The levels of  $\beta$ -RA were quantified tissue extracts by HPLC-UV. The screening to detect other hydroxybenzoic acid derivate was performed by UPLC-MS/MS.

**Quantification of pro-inflammatory mediators in murine RAW 264.7 macrophages and brainstem extracts**

Concentrations of interleukin (IL)-1 $\beta$ , IL-2, interferon- $\gamma$  (IFN- $\gamma$ ), tumor necrosis factor- $\alpha$  (TNF- $\alpha$ ), and growth regulated oncogene- $\alpha$  (GRO- $\alpha$ ) were quantified in duplicates in the supernatant of the cell culture of murine RAW 264.7 macrophages and brainstem tissue using ProcartaPlex™ Multiplex immunoassays (eBioscience), as previously described and according to the manufacturer instructions (Hinz *et al*, 2000; Reichmann *et al*, 2015).

**Statistical analysis**

Number of animals in each group were calculated in order to detect gross ~60% changes in the biomarkers measurements (based upon  $\alpha = 0.05$  and power of  $\beta = 0.8$ ). We used the application available in: <http://www.biomath.info/power/index.htm>. Animals were genotyped and randomly assigned in experimental groups in separate cages by the technician of the animal facility. Data are expressed as the mean  $\pm$  SD of 6–10 experiments per group. A one-way ANOVA with a Tukey's *post hoc* test was used to compare the differences between three experimental groups. Studies with two experimental groups were evaluated using unpaired Student's *t*-test. A *P*-value of  $< 0.05$  was considered to be statistically significant. A Mann–Whitney *U*-test was used for the statistic analysis of the hormones measurements. Survival curve was analyzed by log-rank (Mantel-Cox) and the Gehan–Breslow–Wilcoxon tests.

**Data and software availability**

RNA-Seq data were generated as described above. The files have been uploaded in the repository Gene Expression Omnibus. The accession number is GSE120287. All data can be found at <https://www.ncbi.nlm.nih.gov/geo/query/acc.cgi?acc=GSE120287>.

**Expanded View** for this article is available online.

**Acknowledgements**

We thank Stacy Kelly Aguirre for the English editing. We are grateful to Ana Fernandez (Universidad de Granada) and Samuel Cantarero (Universidad de Granada) for their technical support at the facilities of bioanalysis, MRI and MS. We thank Dr. Catarina M. Quinzii for the critical review of the study. This work was supported by grants from Ministerio de Economía y Competitividad, Spain, and the ERDF (grant numbers SAF2013-47761-R and SAF2015-65786-R), from the NIH (P01HD080642), and from the University of Granada (grant reference “UNETE”, UCE-PP2017-06). A.H.-G. is a “FPU fellow” from the Ministerio de Educación Cultura y Deporte, Spain. E.B.-C. and M.E.D.-C. were supported by the Junta de Andalucía. L.C.L. was supported by the “Ramón y Cajal” National Programme, Ministerio de Economía y Competitividad, Spain (RYC-2011-07643). The results shown in this article will constitute a section of the A.H.-G. doctoral thesis at the University of Granada.

**Author contributions**

AH-G led the study, developed the survival assay and the body weight measurement, and conducted WB assays, the tests to assess the mitochondrial bioenergetics, HPLC analysis, luminex assays, immunohistochemistry assays, analyzed the results, designed the figures, and wrote the manuscript.

EB-C collected the data for the survival curve and the body weight representation, performed the work in the RAW cells, contributed to the mitochondrial assays, managed the mouse colony, and critically reviewed the manuscript. MB designed and analyzed the RNA-Seq and contributed to the discussion. MED-C developed the assays with zebrafish embryos and critically reviewed the manuscript. LS-M ran some WB in the kidneys and heart. MR and JD measured the blood pressure and heart rate. RKS performed the COX and SDH assays in muscle. CP measured the levels of the steroid hormones. GE and DA-C contributed to the discussion. LCL conceived the idea for the project, supervised the experiments, and edited the manuscript. All authors critically reviewed the manuscript. The results shown in this article will constitute a section of the AH-G doctoral thesis at the University of Granada.

### Conflict of interest

A.H.-G., E.B.-C., M.B., and L.C.L. are inventors on a patent application entitled "Pharmacological Composition for the Treatment of Diseases Associated to a Deficiency in the Endogenous Cellular Synthesis of Coenzyme Q9 and Coenzyme Q10".

### For more information

- (i) Online Mendelian Inheritance in Man (OMIM) COQ9: *S. cerevisiae*, homolog of; COQ9: <http://omim.org/entry/612837#0001>
- (ii) International mito-patients: <http://www.mitopatients.org/index.html>
- (iii) The association of mitochondrial disease patients in Spain: <http://www.aepmi.org/publicoIngles/index.php>
- (iv) The United Mitochondrial Disease Foundation: <http://www.umdf.org/>

## References

- Adams TB, Cohen SM, Doull J, Feron VJ, Goodman JI, Marnett LJ, Munro IC, Portoghese PS, Smith RL, Waddell WJ *et al* (2005) The FEMA GRAS assessment of hydroxy- and alkoxy-substituted benzyl derivatives used as flavor ingredients. *Food Chem Toxicol* 43: 1241–1271
- Arroyo A, Santos-Ocana C, Ruiz-Ferrer M, Padilla S, Gavilan A, Rodriguez-Aguilera JC, Navas P (2006) Coenzyme Q is irreplaceable by demethoxy-coenzyme Q in plasma membrane of *Caenorhabditis elegans*. *FEBS Lett* 580: 1740–1746
- Bentinger M, Dallner G, Chojnacki T, Swiezewska E (2003) Distribution and breakdown of labeled coenzyme Q10 in rat. *Free Radic Biol Med* 34: 563–575
- Bhagavan HN, Chopra RK (2007) Plasma coenzyme Q10 response to oral ingestion of coenzyme Q10 formulations. *Mitochondrion* 7(Suppl): S78–S88
- Brzywczy J, Sienko M, Kucharska A, Paszewski A (2002) Sulphur amino acid synthesis in *Schizosaccharomyces pombe* represents a specific variant of sulphur metabolism in fungi. *Yeast* 19: 29–35
- Butterworth RF (2015) Pathogenesis of hepatic encephalopathy and brain edema in acute liver failure. *J Clin Exp Hepatol* 5: S96–S103
- Cameron AR, Logie L, Patel K, Bacon S, Forteath C, Harthill J, Roberts A, Sutherland C, Stewart D, Viollet B *et al* (2016) Investigation of salicylate hepatic responses in comparison with chemical analogues of the drug. *Biochim Biophys Acta* 1862: 1412–1422
- Colombo E, Farina C (2016) Astrocytes: key regulators of neuroinflammation. *Trends Immunol* 37: 608–620
- Danhauser K, Herebian D, Haack TB, Rodenburg RJ, Strom TM, Meitinger T, Klee D, Mayatepek E, Prokisch H, Distelmaier F (2016) Fatal neonatal encephalopathy and lactic acidosis caused by a homozygous loss-of-function variant in COQ9. *Eur J Hum Genet* 24: 450–454
- Di Meo I, Fagioli G, Prella A, Viscomi C, Zeviani M, Tiranti V (2011) Chronic exposure to sulfide causes accelerated degradation of cytochrome c oxidase in ethylmalonic encephalopathy. *Antioxid Redox Signal* 15: 353–362
- Di Meo I, Marchet S, Lamperti C, Zeviani M, Viscomi C (2017) AAV9-based gene therapy partially ameliorates the clinical phenotype of a mouse model of Leigh syndrome. *Gene Ther* 24: 661–667
- Diaz F, Garcia S, Padgett KR, Moraes CT (2012) A defect in the mitochondrial complex III, but not complex IV, triggers early ROS-dependent damage in defined brain regions. *Hum Mol Genet* 21: 5066–5077
- Diaz-Casado ME, Rusanova I, Aranda P, Fernandez-Ortiz M, Sayed RKA, Fernandez-Gil BI, Hidalgo-Gutierrez A, Escames G, Lopez LC, Acuna-Castroviejo D (2018) *In vivo* determination of mitochondrial respiration in 1-Methyl-4-Phenyl-1,2,3,6-Tetrahydropyridine-treated Zebrafish reveals the efficacy of melatonin in restoring mitochondrial normalcy. *Zebrafish* 15: 15–26
- DiMauro S, Quinzii CM, Hirano M (2007) Mutations in coenzyme Q10 biosynthetic genes. *J Clin Invest* 117: 587–589
- DiMauro S, Schon EA, Carelli V, Hirano M (2013) The clinical maze of mitochondrial neurology. *Nat Rev Neurol* 9: 429–444
- Doimo M, Trevisson E, Airik R, Bergdoll M, Santos-Ocana C, Hildebrandt F, Navas P, Pierrel F, Salvati L (2014) Effect of vanillic acid on COQ6 mutants identified in patients with coenzyme Q deficiency. *Biochim Biophys Acta* 1842: 1–6
- Duncan AJ, Bitner-Glindzic M, Meunier B, Costello H, Hargreaves IP, Lopez LC, Hirano M, Quinzii CM, Sadowski MI, Hardy J *et al* (2009) A nonsense mutation in COQ9 causes autosomal-recessive neonatal-onset primary coenzyme Q10 deficiency: a potentially treatable form of mitochondrial disease. *Am J Hum Genet* 84: 558–566
- Emmanuele V, Lopez LC, Berardo A, Naini A, Tadesse S, Wen B, D'Agostino E, Solomon M, DiMauro S, Quinzii C *et al* (2012) Heterogeneity of coenzyme Q10 deficiency: patient study and literature review. *Arch Neurol* 69: 978–983
- Eto K, Asada T, Arima K, Makifuchi T, Kimura H (2002) Brain hydrogen sulfide is severely decreased in Alzheimer's disease. *Biochem Biophys Res Commun* 293: 1485–1488
- Fazakerley DJ, Chaudhuri R, Yang P, Maghazal GJ, Thomas KC, Krycer JR, Humphrey SJ, Parker BL, Fisher-Wellman KH, Meoli CC *et al* (2018) Mitochondrial CoQ deficiency is a common driver of mitochondrial oxidants and insulin resistance. *Elife* 7: e32111
- Fernandez-Vizarra E, Lopez-Perez MJ, Enriquez JA (2002) Isolation of biogenetically competent mitochondria from mammalian tissues and cultured cells. *Methods* 26: 292–297
- Freyer C, Stranneheim H, Naess K, Mourier A, Felser A, Maffezzini C, Lesko N, Bruhn H, Engvall M, Wibom R *et al* (2015) Rescue of primary ubiquinone deficiency due to a novel COQ7 defect using 2,4-dihydroxybenzoic acid. *J Med Genet* 52: 779–783
- Garcia-Corzo L, Luna-Sanchez M, Doerrier C, Garcia JA, Guaras A, Acin-Perez R, Bulles-Peregrin J, Lopez A, Escames G, Enriquez JA *et al* (2013) Dysfunctional Coq9 protein causes predominant encephalomyopathy associated with CoQ deficiency. *Hum Mol Genet* 22: 1233–1248
- Garcia-Corzo L, Luna-Sanchez M, Doerrier C, Ortiz F, Escames G, Acuna-Castroviejo D, Lopez LC (2014) Ubiquinol-10 ameliorates mitochondrial encephalopathy associated with CoQ deficiency. *Biochim Biophys Acta* 1842: 893–901
- Gigante G, Diella S, Santangelo L, Trevisson E, Acosta MJ, Amatruda M, Finzi G, Caridi G, Murer L, Accetturo M *et al* (2017) Further phenotypic heterogeneity of CoQ10 deficiency associated with steroid resistant nephrotic syndrome and novel COQ2 and COQ6 variants. *Clin Genet* 92: 224–226

- Gomez-Guzman M, Jimenez R, Romero M, Sanchez M, Zarzuelo MJ, Gomez-Morales M, O'Valle F, Lopez-Farre AJ, Algieri F, Galvez J *et al* (2014) Chronic hydroxychloroquine improves endothelial dysfunction and protects kidney in a mouse model of systemic lupus erythematosus. *Hypertension* 64: 330–337
- Heeringa SF, Chernin G, Chaki M, Zhou W, Sloan AJ, Ji Z, Xie LX, Salvati L, Hurd TW, Vega-Warner V *et al* (2011) COQ6 mutations in human patients produce nephrotic syndrome with sensorineural deafness. *J Clin Invest* 121: 2013–2024
- Herebian D, Lopez LC, Distelmaier F (2017a) Bypassing human CoQ10 deficiency. *Mol Genet Metab* 123: 289–291
- Herebian D, Seibt A, Smits SHJ, Bunning G, Freyer C, Prokisch H, Karall D, Wredenberg A, Wedell A, Lopez LC *et al* (2017b) Detection of 6-demethoxyubiquinone in CoQ10 deficiency disorders: insights into enzyme interactions and identification of potential therapeutics. *Mol Genet Metab* 121: 216–223
- Herebian D, Seibt A, Smits SHJ, Rodenburg RJ, Mayatepek E, Distelmaier F (2017c) 4-Hydroxybenzoic acid restores CoQ10 biosynthesis in human COQ2 deficiency. *Ann Clin Transl Neurol* 4: 902–908
- Hine C, Harputlugil E, Zhang Y, Ruckenstein C, Lee BC, Brace L, Longchamp A, Trevino-Villarreal JH, Mejia P, Ozaki CK *et al* (2015) Endogenous hydrogen sulfide production is essential for dietary restriction benefits. *Cell* 160: 132–144
- Hinz B, Kraus V, Pahl A, Brune K (2000) Salicylate metabolites inhibit cyclooxygenase-2-dependent prostaglandin E(2) synthesis in murine macrophages. *Biochem Biophys Res Commun* 274: 197–202
- Hughes BG, Harrison PM, Hekimi S (2017) Estimating the occurrence of primary ubiquinone deficiency by analysis of large-scale sequencing data. *Sci Rep* 7: 17744
- Ignatenko O, Chilov D, Paetau I, de Miguel E, Jackson CB, Capin G, Paetau A, Terzioglu M, Euro L, Suomalainen A (2018) Loss of mtDNA activates astrocytes and leads to spongiform encephalopathy. *Nat Commun* 9: 70
- Johnson SC, Yanos ME, Kayser EB, Quintana A, Sangesland M, Castanza A, Uhde L, Hui J, Wall VZ, Gagnidze A *et al* (2013) mTOR inhibition alleviates mitochondrial disease in a mouse model of Leigh syndrome. *Science* 342: 1524–1528
- Kawamukai M (2016) Biosynthesis of coenzyme Q in eukaryotes. *Biosci Biotechnol Biochem* 80: 23–33
- Kuhl I, Miranda M, Atanassov I, Kuznetsova I, Hinz Y, Mourier A, Filipovska A, Larsson NG (2017) Transcriptomic and proteomic landscape of mitochondrial dysfunction reveals secondary coenzyme Q deficiency in mammals. *Elife* 6: e30952
- Lan X, Liu R, Sun L, Zhang T, Du G (2011) Methyl salicylate 2-O-beta-D-lactoside, a novel salicylic acid analogue, acts as an anti-inflammatory agent on microglia and astrocytes. *J Neuroinflammation* 8: 98
- Lax NZ, Campbell GR, Reeve AK, Ohno N, Zamboni J, Blakely EL, Taylor RW, Bonilla E, Tanji K, DiMauro S *et al* (2012) Loss of myelin-associated glycoprotein in kerns-sayre syndrome. *Arch Neurol* 69: 490–499
- Li H, Handsaker B, Wysoker A, Fennell T, Ruan J, Homer N, Marth G, Abecasis G, Durbin R, 1000 Genome Project Data Processing Subgroup (2009) The Sequence Alignment/Map format and SAMtools. *Bioinformatics* 25: 2078–2079
- Liddel S, Barres B (2015) SnapShot: astrocytes in health and disease. *Cell* 162: 1170 e1171
- Liddel SA, Barres BA (2017) Reactive astrocytes: production, function, and therapeutic potential. *Immunity* 46: 957–967
- Linden DR, Furne J, Stoltz GJ, Abdel-Rehim MS, Levitt MD, Szurszewski JH (2012) Sulphide quinone reductase contributes to hydrogen sulphide metabolism in murine peripheral tissues but not in the CNS. *Br J Pharmacol* 165: 2178–2190
- Lohman DC, Forouhar F, Beebe ET, Stefely MS, Minogue CE, Ulbrich A, Stefely JA, Sukumar S, Luna-Sanchez M, Jochem A *et al* (2014) Mitochondrial COQ9 is a lipid-binding protein that associates with COQ7 to enable coenzyme Q biosynthesis. *Proc Natl Acad Sci USA* 111: E4697–E4705
- Lopez LC, Schuelke M, Quinzii CM, Kanki T, Rodenburg RJ, Naini A, DiMauro S, Hirano M (2006) Leigh syndrome with nephropathy and CoQ10 deficiency due to decaprenyl diphosphate synthase subunit 2 (PDSS2) mutations. *Am J Hum Genet* 79: 1125–1129
- Lopez LC, Quinzii CM, Area E, Naini A, Rahman S, Schuelke M, Salvati L, DiMauro S, Hirano M (2010) Treatment of CoQ(10) deficient fibroblasts with ubiquinone, CoQ analogs, and vitamin C: time- and compound-dependent effects. *PLoS One* 5: e11897
- Luna-Sanchez M, Diaz-Casado E, Barca E, Tejada MA, Montilla-Garcia A, Cobos EJ, Escames G, Acuna-Castroviejo D, Quinzii CM, Lopez LC (2015) The clinical heterogeneity of coenzyme Q10 deficiency results from genotypic differences in the Coq9 gene. *EMBO Mol Med* 7: 670–687
- Luna-Sanchez M, Hidalgo-Gutiérrez A, Hildebrandt TM, Chaves-Serrano J, Barriocanal-Casado E, Santos-Fandila A, Romero M, Sayed RK, Duarte J, Prokisch H *et al* (2017) CoQ deficiency causes disruption of mitochondrial sulfide oxidation, a new pathomechanism associated with this syndrome. *EMBO Mol Med* 9: 78–95
- Mayo L, Trauger SA, Blain M, Nadeau M, Patel B, Alvarez JI, Mascanfroni ID, Yeste A, Kivisakk P, Kallas K *et al* (2014) Regulation of astrocyte activation by glycolipids drives chronic CNS inflammation. *Nat Med* 20: 1147–1156
- Miranda AS, Cordeiro TM, Dos Santos Lacerda Soares TM, Ferreira RN, Simoes ESAC (2017) Kidney-brain axis inflammatory cross-talk: from bench to bedside. *Clin Sci (Lond)* 131: 1093–1105
- Mishanina TV, Libiad M, Banerjee R (2015) Biogenesis of reactive sulfur species for signaling by hydrogen sulfide oxidation pathways. *Nat Chem Biol* 11: 457–464
- Nunnari J, Suomalainen A (2012) Mitochondria: in sickness and in health. *Cell* 148: 1145–1159
- Ozeir M, Muhlenhoff U, Weber H, Lill R, Fontecave M, Pierrel F (2011) Coenzyme Q biosynthesis: Coq6 is required for the C5-hydroxylation reaction and substrate analogs rescue Coq6 deficiency. *Chem Biol* 18: 1134–1142
- Pagliarini DJ, Calvo SE, Chang B, Sheth SA, Vafai SB, Ong SE, Walford GA, Sugiana C, Boneh A, Chen WK *et al* (2008) A mitochondrial protein compendium elucidates complex I disease biology. *Cell* 134: 112–123
- Pierrel F (2017) Impact of chemical analogs of 4-hydroxybenzoic acid on coenzyme Q biosynthesis: from inhibition to bypass of coenzyme Q deficiency. *Front Physiol* 8: 436
- Quintana A, Kruse SE, Kapur RP, Sanz E, Palmiter RD (2010) Complex I deficiency due to loss of Ndufs4 in the brain results in progressive encephalopathy resembling Leigh syndrome. *Proc Natl Acad Sci USA* 107: 10996–11001
- Reichmann F, Hassan AM, Farzi A, Jain P, Schuligoi R, Holzer P (2015) Dextran sulfate sodium-induced colitis alters stress-associated behaviour and neuropeptide gene expression in the amygdala-hippocampus network of mice. *Sci Rep* 5: 9970
- Ribas V, Garcia-Ruiz C, Fernandez-Checa JC (2014) Glutathione and mitochondria. *Front Pharmacol* 5: 151
- Rogers GW, Brand MD, Petrosyan S, Ashok D, Elorza AA, Ferrick DA, Murphy AN (2011) High throughput microplate respiratory measurements using minimal quantities of isolated mitochondria. *PLoS One* 6: e21746

- Rothhammer V, Mascanfroni ID, Bunse L, Takenaka MC, Kenison JE, Mayo L, Chao CC, Patel B, Yan R, Blain M *et al* (2016) Type I interferons and microbial metabolites of tryptophan modulate astrocyte activity and central nervous system inflammation via the aryl hydrocarbon receptor. *Nat Med* 22: 586–597
- Rothhammer V, Kenison JE, Tjon E, Takenaka MC, de Lima KA, Borucki DM, Chao CC, Wilz A, Blain M, Healy L *et al* (2017) Sphingosine 1-phosphate receptor modulation suppresses pathogenic astrocyte activation and chronic progressive CNS inflammation. *Proc Natl Acad Sci USA* 114: 2012–2017
- Smith AC, Ito Y, Ahmed A, Schwartzentruber JA, Beaulieu CL, Aberg E, Majewski J, Bulman DE, Horsting-Wethly K, Koning DV *et al* (2018) A family segregating lethal neonatal coenzyme Q10 deficiency caused by mutations in COQ9. *J Inherit Metab Dis* 41: 719–729
- Suomalainen A, Elo JM, Pietilainen KH, Hakonen AH, Sevastianova K, Korpela M, Isohanni P, Marjavaara SK, Tyni T, Kiuru-Enari S *et al* (2011) FGF-21 as a biomarker for muscle-manifesting mitochondrial respiratory chain deficiencies: a diagnostic study. *Lancet Neurol* 10: 806–818
- Tanji K, Bonilla E (2008) Light microscopic methods to visualize mitochondria on tissue sections. *Methods* 46: 274–280
- Tegelberg S, Tomasic N, Kallijarvi J, Purhonen J, Elmer E, Lindberg E, Nord DG, Soller M, Lesko N, Wedell A *et al* (2017) Respiratory chain complex III deficiency due to mutated BCS1L: a novel phenotype with encephalomyopathy, partially phenocopied in a Bcs1l mutant mouse model. *Orphanet J Rare Dis* 12: 73
- Thackeray JT, Hupe HC, Wang Y, Bankstahl JP, Berding G, Ross TL, Bauersachs J, Wollert KC, Bengel FM (2018) Myocardial inflammation predicts remodeling and neuroinflammation after myocardial infarction. *J Am Coll Cardiol* 71: 263–275
- Vafai SB, Mootha VK (2012) Mitochondrial disorders as windows into an ancient organelle. *Nature* 491: 374–383
- Wang Y, Ozer D, Hekimi S (2015) Mitochondrial function and lifespan of mice with controlled ubiquinone biosynthesis. *Nat Commun* 6: 6393
- Wang W, Karamanlidis G, Tian R (2016) Novel targets for mitochondrial medicine. *Sci Transl Med* 8: 326rv323
- Wang Y, Smith C, Parboosingh JS, Khan A, Innes M, Hekimi S (2017) Pathogenicity of two COQ7 mutations and responses to 2,4-dihydroxybenzoate bypass treatment. *J Cell Mol Med* 21: 2329–2343
- Xie LX, Ozeir M, Tang JY, Chen JY, Kieffer-Jaquinod S, Fontecave M, Clarke CF, Pierrel F (2012) Over-expression of the Coq8 kinase in *Saccharomyces cerevisiae* coq null mutants allows for accumulation of diagnostic intermediates of the Coenzyme Q6 biosynthetic pathway. *J Biol Chem* 287: 23571–23581
- Yang YY, Vasta V, Hahn S, Gangoiti JA, Opheim E, Sedensky MM, Morgan PG (2011) The role of DMQ(9) in the long-lived mutant clk-1. *Mech Ageing Dev* 132: 331–339
- Yoo SE, Chen L, Na R, Liu Y, Rios C, Van Remmen H, Richardson A, Ran Q (2012) Gpx4 ablation in adult mice results in a lethal phenotype accompanied by neuronal loss in brain. *Free Radic Biol Med* 52: 1820–1827
- Zamanian JL, Xu L, Foo LC, Nouri N, Zhou L, Giffard RG, Barres BA (2012) Genomic analysis of reactive astrogliosis. *J Neurosci* 32: 6391–6410



**License:** This is an open access article under the terms of the Creative Commons Attribution 4.0 License, which permits use, distribution and reproduction in any medium, provided the original work is properly cited.